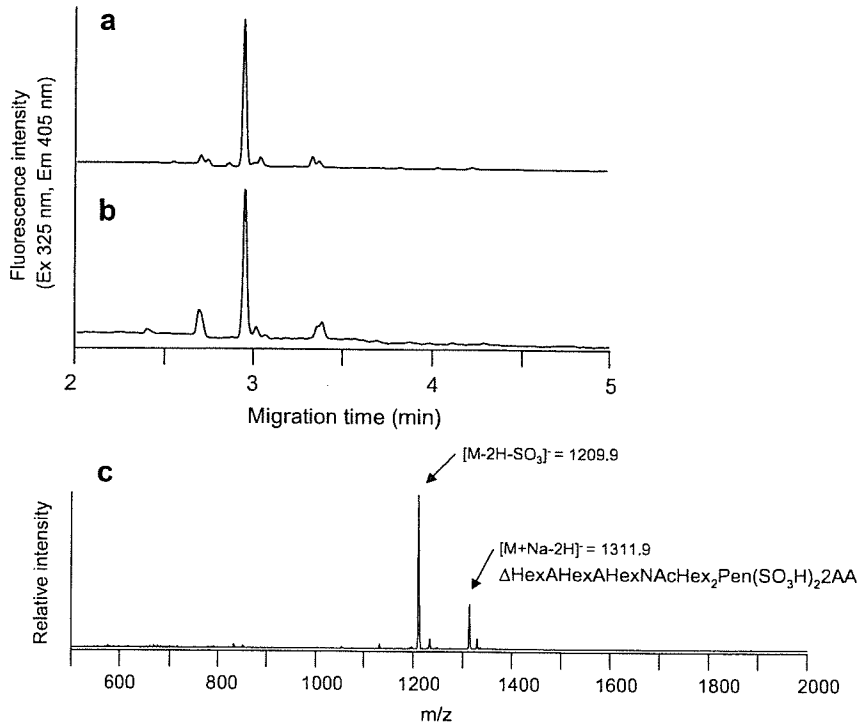

Fig. 3. CE and MALDI-TOF MS analysis of 2AA-labeled linkage oligosaccharides derived from UTI. 2AA-labeled oligosaccharides released by AGC (a) and the conventional in-tube method (b) were analyzed by CE. Analytical conditions for CE; capillary, DB-1 capillary (30 cm × 100 μm i.d.); running buffer, 100 mM Tris–borate buffer (pH 8.0) containing 10% PEG70000; applied voltage, 20 kV; injection, pressure method (1.0 psi for 10 s); temperature, 25 °C; detection, helium–cadmium laser-induced fluorescence (Ex: 325 nm, Em: 405 nm). (c) MALDI-TOF MS spectra of 2AA-labeled linkage oligosaccharides.

hexasaccharides derived from the linkage region of bovine nasal septal cartilage PG were sulfated at either the C4 or the C6 position of the GalNAc residue [11]. Accordingly, we concluded that peak **3**, which was resistant to chondro-4-sulfatase, is hexasaccharide sulfated at the C6 position of the GalNAc residue. Structures of the linkage hexasaccharides observed in BNC–PG are summarized and relative abundances of glycans estimated from their peak areas in CE analysis are shown in Table 1. The relative abundances of glycans observed in BNC–PG were slightly different from those reported previously [11]. The reasons for this difference may be due to the difference of PG material used because de Beer et al. [11] used a more limited part of nasal cartilage (septal) as a source of PG, while KS chains in BNC–PG were not observed in the present study and further studies are required.

Aggrecan is the major proteoglycan in articular cartilage and is important for proper functioning of articular cartilage. Aggrecan derived from bovine articular cartilage has chondroitin-6-sulfate chains as major GAGs, and their linkage-region oligosaccharides were sulfated at the C6 position predominantly [15,16]. We released the oligosaccharides at the linkage region of aggrecan by AGC and analyzed them after labeling with 2AA (Fig. 5). Two major peaks were observed at 3.4 and 4.1 min (Fig. 5a). The glycan (peak **1**) has one sulfate group in the molecule. These peaks were not digested with chondro-4-sulfatase and calf intestine alkaline phosphatase (data not shown). Thus, we concluded that peaks **1** and **2** are hexasaccharides having a sulfate group at the C6 position of the GalNAc residue and nonsulfated hexasaccharide, respectively. This result was also supported by MALDI-TOF MS analysis (Fig. 5b). The oligosaccharides derived from the linkage region of aggrecan showed an abundant ion at *m/z* 1209.6 of monosulfated hexasacchride (ΔHexAHexAHexNAcHex$_2$Pen(SO$_3$H)2AA) with its sodium adduct ion (*m/z* 1232) and a small ion peak at *m/z* 1129.3 of nonsulfated hexasaccharide (ΔHexAHexAHexNAcHex$_2$Pen2AA). The structures and relative abundances of these hexasaccharides are also summarized in Table 1. Relative abundances of hexasaccharides at the linkage region observed in aggrecan also showed values slightly different from those reported previously [16].

Decorin, which is a member of the small leucine-rich PG family, plays a key role as a modulator of cell growth by interaction with matrix components or a variety of other proteins such as fibronectin or transforming growth factor-β [36]. Recently, decorin was reported to increase in human colon adenocarcinomas with significant structure changes [6]. Mammalian decorin has a single CS/DS chain that is attached to Ser4 [37]. We analyzed the oligosaccharides at the linkage region of the CS/DS chain of decorin

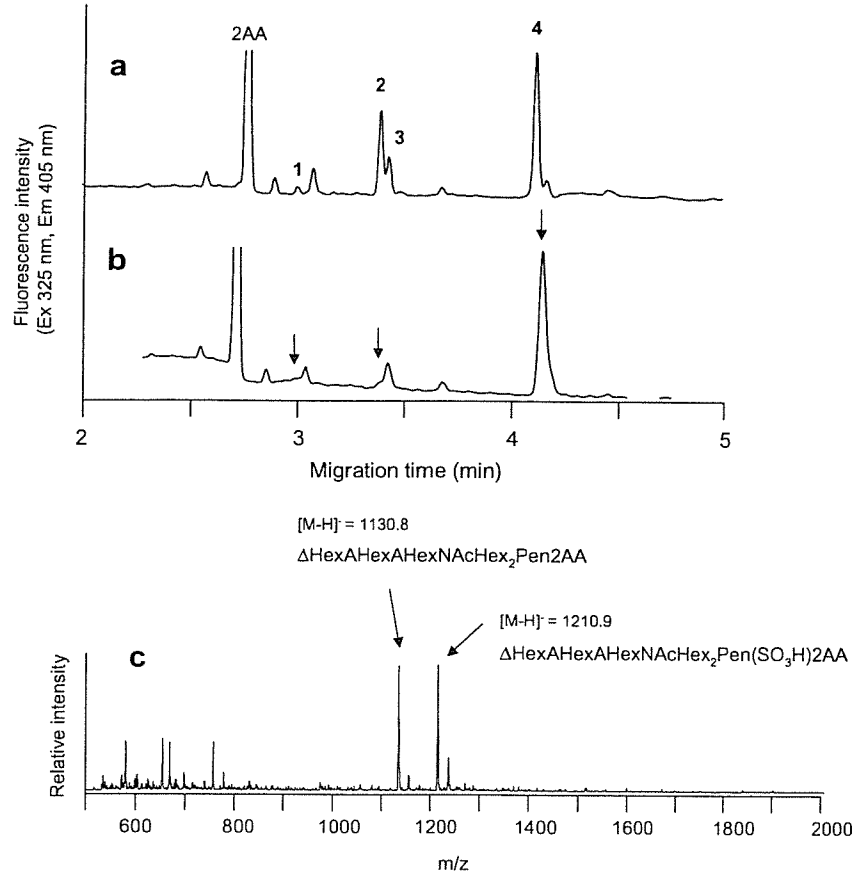

Fig. 4. CE and MALDI-TOF MS analysis of 2AA-labeled linkage oligosaccharides derived from BNC–PG. 2AA-labeled linkage oligosaccharides derived from BNC–PG were analyzed by CE before digestion (a) and after digestion with chondro-4-sulfatase (b). Analytical conditions for CE were the same as those described in Fig. 3. Arrows indicate the peaks changed after digestion. (c) MALDI-TOF MS spectra of 2AA-labeled linkage oligosaccharides.

derived from bovine articular cartilage. The results of CE and MALDI-TOF MS analysis are shown in Fig. 6. In CE analysis of the 2AA-labeled oligosaccharides, monosulfated hexasaccharides (peaks **2** and **3**) and nonsulfated hexasaccharide (peak **4**) were observed at 3.3 and 4.3 min, respectively, as major components (Fig. 6a). A broad peak (peak **1**) due to disulfated hexasaccharides was also observed at ca. 2.7 min as minor components. After digestion with chondro-4-sulfatase, peak **2** was shifted to the position of peak **4** (Fig. 6b) but peak **3** was not digested with alkaline phosphatase (data not shown). These results clearly indicated that peaks **2** and **3** were the C4 and C6 sulfated hexasaccharide, respectively. After digestion with chondroitinase AC-II, the 2AA-labeled linkage oligosaccharides gave two peaks at 3.3 and 4.3 min, respectively (Fig. 6c). The major peak observed at 4.3 min seems to be the linkage tetrasaccharide ΔHexAβ1-3Galβ1-3Galβ1-4Xyl-2AA from its migration time. A portion of the minor peak observed at 3.3 min, which is resistant to chondroitinase AC-II, is probably due to iduronic acid-containing hexasaccharide because chondroitinase AC-II does not act on this hexasaccharide [38]. This type of oligosaccharide which contains iduronic acid was also found in recombinant decorin expressed in Chinese hamster ovary cells [39]. MALDI-TOF MS analysis showed a molecular ion at *m/z* 1210.9 corresponding to monosulfated hexasaccharides (ΔHexAHexAHexNAcHex$_2$Pen(SO$_3$H)2AA) and a minor ion at *m/z* 1130.9 due to nonsulfated hexasaccharide (ΔHexAHexAHexNAcHex$_2$Pen2AA) (Fig. 6d). The results are summarized in Table 1. The broad peak (peak **1**) of disulfated hexasaccharides indicates that the sulfation patterns of disulfated hexasaccharides are highly heterogenous.

Biglycan is also a member of the small leucine-rich PG family and usually has two CS/DS chains attached to Ser5 and Ser11 [40]. We analyzed the oligosaccharides at the linkage region of CS/DS chains of biglycan derived from bovine articular cartilage and compared them with those of decorin. The results are shown in Fig. 7. In CE analysis, the oligosaccharides derived from biglycan showed an electropherogram similar to that observed for the analysis of oligosaccharides derived from decorin (Fig. 7a), but the oligosaccharide composition was different from that of decorin. After digestion with chondro-4-sulfatase, peak **2** disappeared and peak **4** increased (Fig. 7b) but peak **3** was not digested with alkaline phosphatase (data

Table 1
Structures and relative abundances of linkage oligosaccharides derived from PGs

Peak No.[a]	Structure[b]	Relative abundance (%)[c]
BNC–PG		
1	ΔHexAα1-3GalNAc(4S)β1-4GlcAβ1-3Gal(4S)β1-3Galβ1-4Xyl-2AA	2 (11)
2	ΔHexAα1-3GalNAc(4S)β1-4GlcAβ1-3Galβ1-3Galβ1-4Xyl-2AA	28 (43)
3	ΔHexAα1-3GalNAc(6S)β1-4GlcAβ1-3Galβ1-3Galβ1-4Xyl-2AA	14 (6)
4	ΔHexAα1-3GalNAcβ1-4GlcAβ1-3Galβ1-3Galβ1-4Xyl-2AA	56 (38)
Aggrecan		
1	ΔHexAα1-3GalNAc(6S)β1-4GlcAβ1-3Galβ1-3Galβ1-4Xyl-2AA	56 (68)
2	ΔHexAα1-3GalNAcβ1-4GlcAβ1-3Galβ1-3Galβ1-4Xyl-2AA	44 (32)
Decorin		
1	ΔHexAα1-3GalNAc(S)β1-4GlcAβ1-3Gal(S)β1-3Galβ1-4Xyl-2AA	21
2	ΔHexAα1-3GalNAc(4S)β1-4GlcAβ1-3Galβ1-3Galβ1-4Xyl-2AA	5
2	ΔHexAα1-3GalNAc(4S)β1-4IdoAα1-3Galβ1-3Galβ1-4Xyl-2AA	16
3	ΔHexAα1-3GalNAc(6S)β1-4GlcAβ1-3Galβ1-3Galβ1-4Xyl-2AA	41
4	ΔHexAα1-3GalNAcβ1-4GlcAβ1-3Galβ1-3Galβ1-4Xyl-2AA	17
Biglycan		
1	ΔHexAα1-3GalNAc(S)β1-4GlcAβ1-3Gal(S)β1-3Galβ1-4Xyl-2AA	10
2	ΔHexAα1-3GalNAc(4S)β1-4GlcAβ1-3Galβ1-3Galβ1-4Xyl-2AA	15
2	ΔHexAα1-3GalNAc(4S)β1-4IdoAα1-3Galβ1-3Galβ1-4Xyl-2AA	1
3	ΔHexAα1-3GalNAc(6S)β1-4GlcAβ1-3Galβ1-3Galβ1-4Xyl-2AA	45
4	ΔHexAα1-3GalNAcβ1-4GlcAβ1-3Galβ1-3Galβ1-4Xyl-2AA	29

[a] Peaks observed in CE analysis.
[b] Previously reported oligosaccharide structure.
[c] Values in parentheses are previously reported.

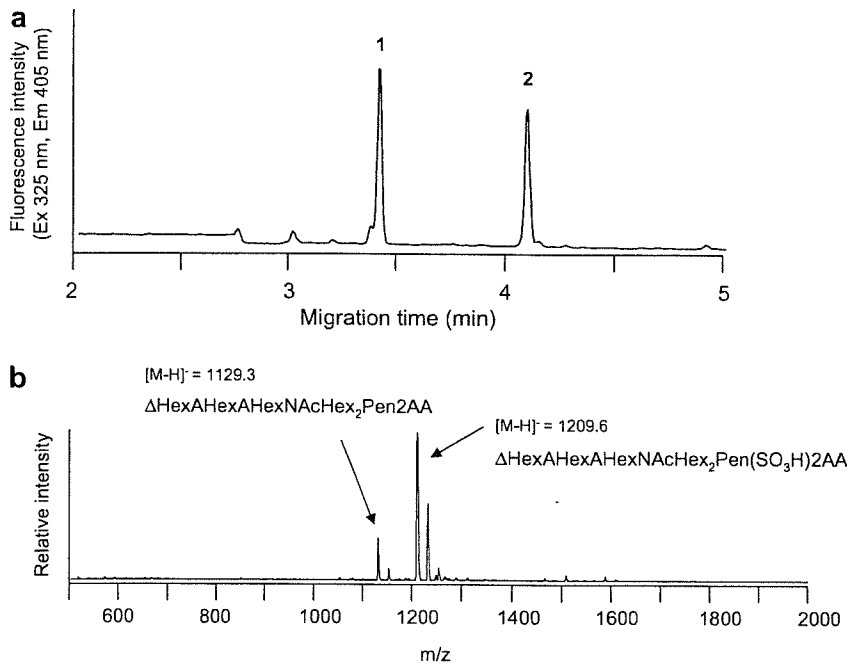

Fig. 5. CE and MALDI-TOF MS analysis of 2AA-labeled linkage oligosaccharides derived from aggrecan. 2AA-labeled linkage oligosaccharides derived from aggrecan were analyzed by CE (a) and MALDI-TOF MS (b). Analytical conditions for CE were the same as those described in Fig. 3.

not shown). After digestion with chondroitinase AC-II, the 2AA-labeled linkage oligosaccharides in biglycan gave a peak at 4.3 min and a small peak of iduronic acid-containing hexasaccharide at 3.3 min (Fig. 7c). In MALDI-TOF MS analysis, the 2AA-labeled linkage oligosaccharides derived from biglycan showed two major molecular ions at *m/z* 1210.3 and *m/z* 1130.1 due to monosulfated hexasaccharides (ΔHexAHexAHexNAcHex$_2$Pen(SO$_3$H)2AA) and nonsulfated hexasaccharide (ΔHexAHexAHexNAcHex$_2$Pen2AA), respectively (Fig. 7d). The list of linkage

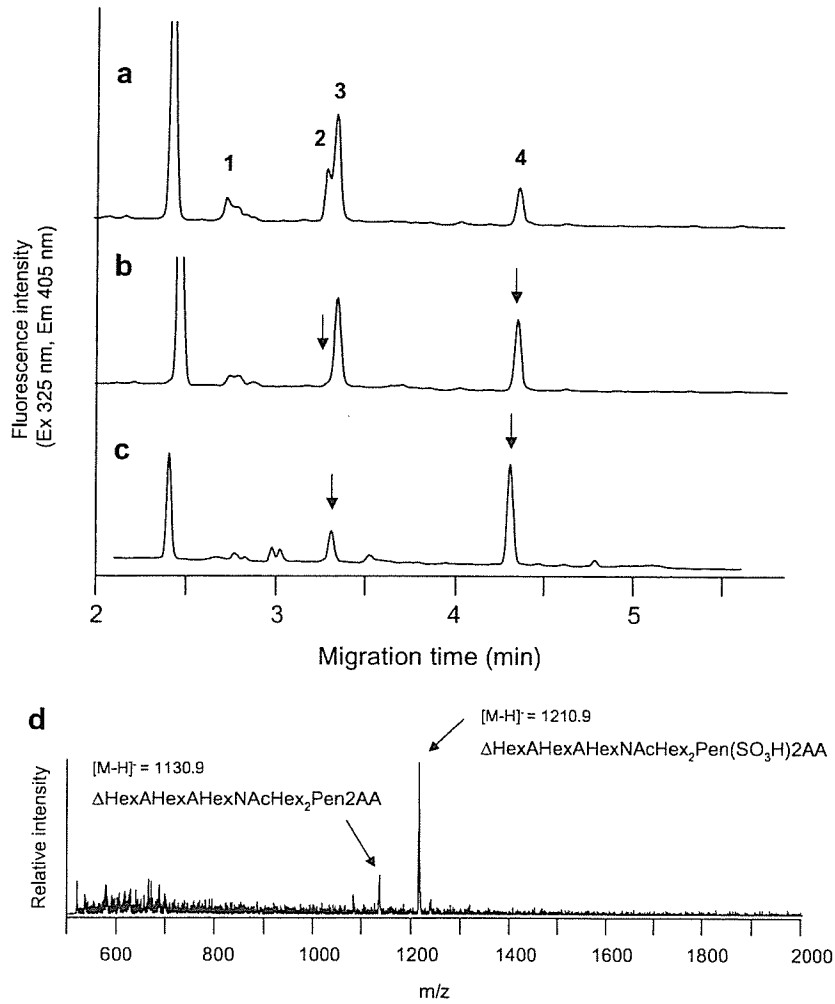

Fig. 6. CE and MALDI-TOF MS analysis of 2AA-labeled linkage oligosaccharides derived from decorin. 2AA-labeled linkage oligosaccharides derived from decorin were analyzed by CE before digestion (a) and after digestion with chondro-4-sulfatase (b) and chondroitinase AC-II (c). Analytical conditions for CE were the same as those described in Fig. 3. Arrows indicate the peaks changed after digestion. (d) MALDI-TOF MS spectra of 2AA-labeled linkage oligosaccharides.

oligosaccharides observed in biglycan is summarized in Table 1.

Disaccharide composition analysis

Disaccharide units of CS chains in PG samples employed in the present study were determined. The mixture of unsaturated disaccharides obtained by digestion with chondroitinase ABC was labeled with AMAC and analyzed by CE according to the procedure described in Fig. 1. The results are shown in Fig. 8. UTI gave two major peaks of Δdi-4S and Δdi-0S at 3.4 and 5.3 min, respectively (Fig. 8a). BNC–PG showed a nearly single peak of Δdi-4S at 3.4 min (Fig. 8b), while aggrecan, decorin and biglycan gave Δdi-6S at 3.3 min and the peak of Δdi-4S (Figs. 8c–e) as the major disaccharides. The disaccharide compositions estimated by peak areas are summarized in Table 2. The relative ratios of disaccharides derived from UTI were 37.2% for Δdi-4S and 62.8% for Δdi-0S. BNC–PG showed a high proportion of Δdi-4S (90.7%), and contained Δdi-6S (9.3%) and a trace amount of Δdi-0S. The major disaccharides derived from aggrecan were Δdi-6S (70.2%), Δdi-4S (21.1%), and Δdi-0S (8.7%). Decorin and biglycan showed both Δdi-4S and Δdi-6S as major components, but biglycan showed higher Δdi-6S content than that observed in decorin. The relative ratios of disaccharides derived from UTI, BNC–PG, and aggrecan showed good agreement with the reported data [11,15,32], but those of disaccharides derived from decorin and biglycan were slightly different [41].

Discussion

We proposed a method for the rapid analysis of oligosaccharides at the GAGs–protein linkage region. To shorten the total time required for the analysis of linkage oligosaccharides in PGs, we fabricated an automatic

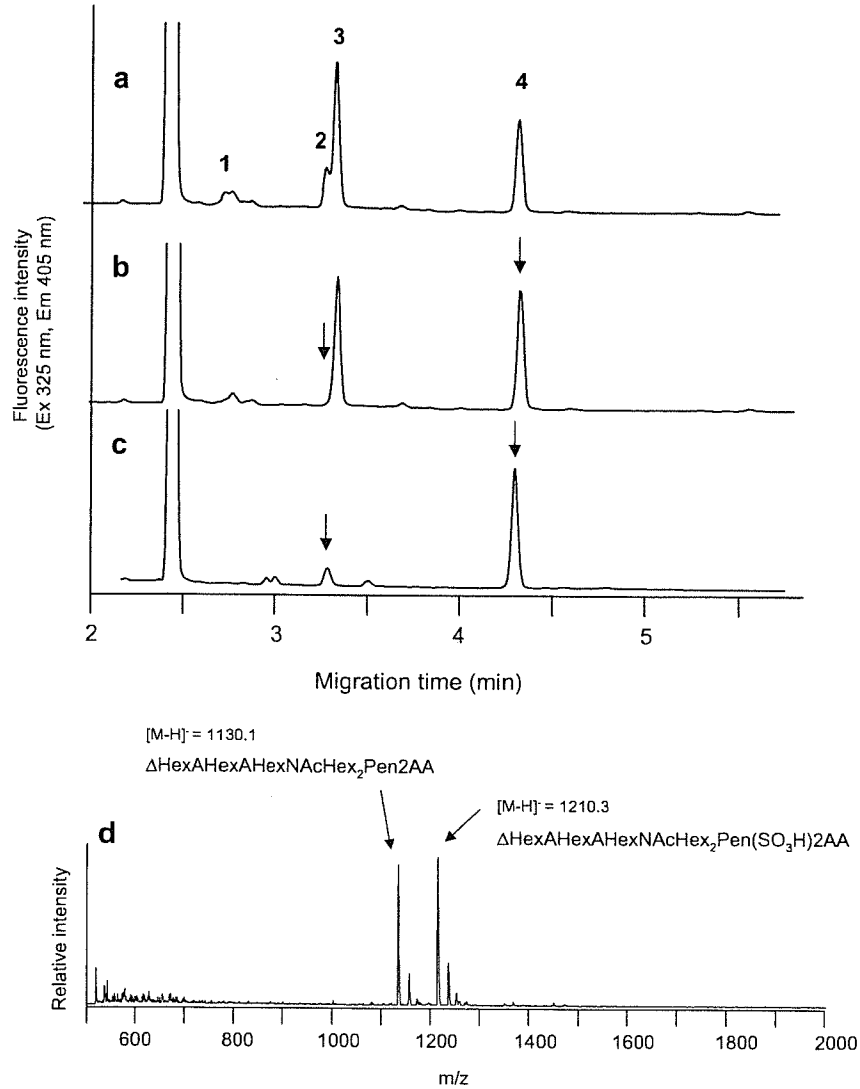

Fig. 7. CE and MALDI-TOF MS analysis of 2AA-labeled linkage oligosaccharides derived from biglycan. 2AA-labeled linkage oligosaccharides derived from biglycan were analyzed by CE (a). (b) and (c) are the results after digestion with chondro-4-sulfatase and chondroitinase AC-II, respectively. Analytical conditions for CE were the same as those described in Fig. 3. Arrows indicate the peaks changed after digestion. (d) MALDI-TOF MS spectra of 2AA-labeled linkage oligosaccharides.

carbohydrate releasing apparatus (AutoGlycoCutter) for rapid release of linkage oligosaccharides by employing the in-line flow system. By using AGC, the time required for release of oligosaccharides is only ca. 3 min, and we can achieve ca. 1000-fold rapid release of oligosaccharides compared to that required by the conventional in-tube method. In addition, it should be noted that analyses of 2AA-labeled oligosaccharides at the linkage region and AMAC-labeled unsaturated disaccharides by CE were completed within 5 and 10 min, respectively. Although the analysis of oligosaccharides at the linkage region has so far been generally performed by HPLC, we demonstrated that CE will be a useful technique. Furthermore, in MALDI-TOF MS analysis, sulfate groups can be lost through fragmentation. Therefore, to analyze the sulfated glycans such as linkage oligosaccharides, it is essential to employ chromatographic techniques such as CE in addition to MALDI-TOF MS. The efficiency of the releasing reaction by the present method was lower than that by the conventional method and was different among the PGs used (57–73% relative to those by the conventional method). However, the profiles obtained by the present method showed separation profiles quite similar to those obtained by the conventional in-tube method. Furthermore, it should be noted that the in-line flow system, in principle, shows excellent reproducibility.

The results of the analysis of linkage oligosaccharide in UTI by a combination of CE and MALDI-TOF MS revealed that AGC could release the linkage oligosaccharides from the protein core without any loss of sulfate groups or degradation of carbohydrate chains due to peeling reaction. We also analyzed the linkage oligosaccharides

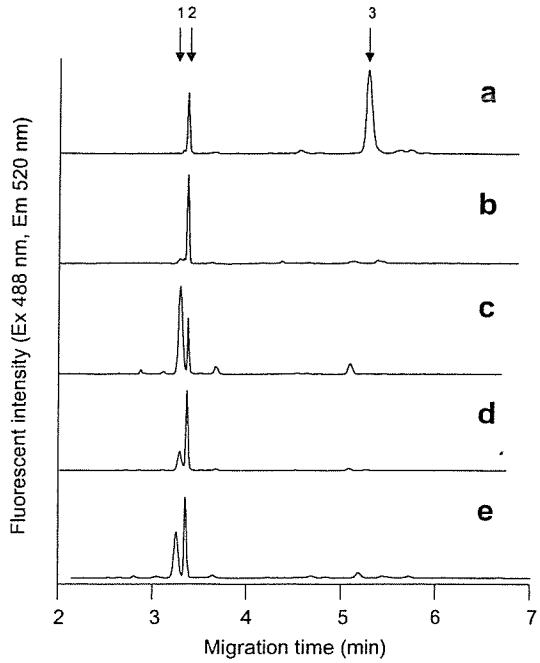

Fig. 8. Disaccharides composition analysis of PGs. AMAC-labeled unsaturated disaccharides derived from (a) UTI, (b) BNC–PG, (c) aggrecan, (d) decorin, and (e) biglycan were analyzed by CE. Analytical conditions for CE; capillary, DB-1 capillary (30 cm × 50 μm i.d.); running buffer, 100 mM Tris–borate buffer (pH 8.0) containing 1% PEG70000; applied voltage, 20 kV; injection, pressure method (1.0 psi for 10 s); temperature, 25 °C; detection, argon-laser-induced fluorescence (Ex: 488 nm, Em: 520 nm). Arrows indicate the migration position of the authentic unsaturated chondro-disaccharides: 1, Δdi-6S; 2, Δdi-4S; 3, Δdi-0S.

Table 2
Disaccharides compositions of PGs

PGs	Disacchride (%)		
	Δdi-6S	Δdi-4S	Δdi-0S
UTI	0	37.2	62.8
BNC–PG	9.3	90.7	Trace
Aggrecan	70.2	21.1	8.7
Decorin	30.4	65.0	3.7
Biglycan	48.9	45.3	5.8

derived from five commercially available CS/DS–PGs to evaluate the performance of AGC.

Because the sulfated Gal structures have not been found in the linkage region of HP/HS–PGs, sulfate groups at the Gal residues are considered to be biological signals for CS/DS biosynthesis. It has been reported that CS chains of BNC–PG contain Δdi-4S unit predominantly [11,35]. Similar results were observed in disaccharide composition analysis (Table 2). In contrast, aggrecan gave more complex mixtures of disaccharides composed of Δdi-6S and Δdi-4S units as major components and small amounts of Δdi-0S unit (Table 2). However, in contrast to the results observed in disaccharides composition analysis, monosulfated hexasaccharides of BNC–PG at the linkage region were those sulfated at both the C4 and the C6 positions of the GalNAc residues (the molar ratio of C4 sulfated and C6 sulfated is ca. 2:1), but the GalNAc residues of aggrecan were sulfated only at the C6 position (Table 1). These results indicated that sulfation patterns observed in the linkage region are markedly different from those observed in the disaccharides repeating region.

It should be noted that BNC–PG and aggrecan also contain keratan sulfate chains mostly attached through *O*-linked glycosides [42]. The core structure of KS is not the PG type but is the mucin type. The nonreducing glycan portions were not eliminated by the digestion with chondroitinases. Accordingly, the released oligosaccharides were not observed by the present method, and further studies may be required for the analysis of KS. In the present study, phosphorylated Xyl structure was not confirmed because the linkage oligosaccharides in CS/DS–PGs used in the present study do not contain this structure [11,15,16,39]. Accordingly, the stability of phosphoesters under the present conditions must be tested in the future.

The results obtained from comparison of the linkage oligosaccharides of decorin with those of biglycan demonstrated that the content of iduronic acid-containing hexasaccharides of biglycan was significantly lower than that of decorin (Table 1). The iduronic acid-containing linkage oligosaccharide is a DS-specific structure [38]. DS is a copolymer of two types of disaccharide unit, which are D-glucuronic acid and L-iduronic acid containing units, and the content of the iduronic acid-containing unit and the sulfation patterns of DS are highly tissue specific. It has been reported that CS/DS chains of decorin and biglycan derived from bovine articular cartilage bear exclusively C4 sulfation [41]. Our results indicate that decorin and biglycan showed high proportions of Δdi-6S, especially biglycan, which are different from the results in the previous report. However, biglycan exhibited a small proportion of the iduronic acid-containing linkage-region oligosaccharide. This observation may correlate with the results of the high proportion of the Δdi-6S.

In the present study, we could not show applications for heparin/heparan sulfate-type PGs because it is difficult to obtain standard samples of heparin/heparan sulfate-type PGs. However, the present method will be applicable to the analysis of heparin/heparan sulfate-type PGs by using a combination of specific enzymes such as heparinase and heparitinase.

In conclusion, the present procedure for the analysis of the glycan part of PGs allows rapid and sensitive analysis of GAGs, will be a powerful tool for routine analysis of PGs, and provides an easy and rapid tool for studying biosynthesis of GAGs.

Acknowledgment

This work was supported by the New Energy and Industrial Technology Development Organization.

References

[1] N.B. Schwartz, Biosynthesis and regulation of expression of proteoglycans, Front. Biosci. 5 (2000) 649–655.

[2] L.Å. Fransson, Structure and function of cell-associated proteoglycans, Trends Biochem. Sci. 12 (1987) 406–411.

[3] L. Ameye, M.F. Young, Mice deficient in small leucine-rich proteoglycans: novel in vivo models for osteoporosis, osteoarthritis, Ehlers-Danlos syndrome, muscular dystrophy, and corneal diseases, Glycobiology 12 (2002) 107R–116R.

[4] E. Forsberg, L. Kjellen, Heparan sulfate: lessons from knockout mice, J. Clin. Invest. 108 (2001) 175–180.

[5] R.V. Iozzo, Matrix proteoglycans: from molecular design to cellular function, Annu. Rev. Biochem. 67 (1998) 609–652.

[6] A.D. Theocharis, Human colon adenocarcinoma is associated with specific post-translational modifications of versican and decorin, Biochim. Biophys. Acta 1588 (2002) 165–172.

[7] R.V. Iozzo, The biology of the small leucine-rich proteoglycans. Functional network of interactive proteins, J. Biol. Chem. 274 (1999) 18843–18846.

[8] K. Sugahara, I. Yamashina, P. de Waard, H. van Halbeek, J.F.G. Vliegenthart, Structural studies on sulfated oligosaccharides from carbohydrate–protein linkage region of chondroitin 4-sulfate proteoglycans of swarm rat chondrosarcoma, J. Biol. Chem. 263 (1988) 10168–10174.

[9] K. Sugahara, H. Kitagawa, Recent advances in the study of the biosynthesis and functions of sulfated glycosaminoglycans, Curr. Opin. Struct. Biol. 10 (2000) 518–527.

[10] K. Sugahara, M. Masuda, T. Harada, I. Yamashina, P. de Waard, J.F.G. Vliegenthart, Structural studies on sulfated oligosaccharides derived from the carbohydrate–protein linkage region of chondroitin sulfate proteoglycans of whale cartilage, Eur. J. Biochem. 202 (1991) 805–811.

[11] T. de Beer, A. Inui, H. Tsuda, K. Sugahara, J.F.G. Vliegenthart, Polydispersity in sulfation profile of oligosaccharide alditols isolated from the protein-linkage region and the repeating disaccharide region of chondroitin 4-sulfate of bovine nasal septal cartilage, Eur. J. Biochem. 240 (1996) 789–797.

[12] F. Cheng, D. Heinegård, L.Å. Fransson, M. Bayliss, J. Bielicki, J. Hopwood, K. Yoshida, Variations in the chondroitin sulfate–protein linkage region of aggrecans from bovine nasal and human articular cartilages, J. Biol. Chem. 271 (1996) 28572–28580.

[13] P. de Waard, J.F.G. Vliegenthart, T. Harada, K. Sugahara, Structural studies on sulfated oligosaccharides derived from the carbohydrate–protein linkage region of chondroitin 6-sulfate proteoglycans of shark cartilage. II. 7 compounds containing 2 or 3 sulfate residues, J. Biol. Chem. 267 (1992) 6036–6043.

[14] K. Sugahara, Y. Ohi, T. Harada, P. de Waard, J.F.G. Vliegenthart, Structural studies on sulfated oligosaccharides derived from the carbohydrate–protein linkage region of chondroitin 6-sulfate proteoglycans of shark cartilage. I. Six compounds containing 0 or 1 sulfate and/or phosphate residues, J. Biol. Chem. 267 (1992) 6027–6035.

[15] R.M. Lauder, T.N. Huckerby, I.A. Nieduszynski, Increased incidence of unsulphated and 4-sulphated residues in the chondroitin sulphate linkage region observed by high-pH anion-exchange chromatography, Biochem. J. 347 (2000) 339–348.

[16] T.N. Huckerby, R.M. Lauder, I.A. Nieduszynski, Structure determination for octasaccharides derived from the carbohydrate–protein linkage region of chondroitin sulphate chains in the proteoglycan aggrecan from bovine articular cartilage, Eur. J. Biochem. 258 (1998) 669–676.

[17] K. Sugahara, S. Yamada, K. Yoshida, P. de Waard, J.F.G. Vliegenthart, A novel sulfated structure in the carbohydrate–protein linkage region isolated from porcine intestinal heparin, J. Biol. Chem. 267 (1992) 1528–1533.

[18] K. Sugahara, R. Tohno-oka, S. Yamada, K.H. Khoo, H.R. Morris, A. Dell, Structural studies on the oligosaccharides isolated from bovine kidney heparan sulphate and characterization of bacterial heparitinase used as substrates, Glycobiology 4 (1994) 535–544.

[19] L.Å. Fransson, I. Silverberg, I. Carlstedt, Structure of the heparan sulfate–protein linkage region. Demonstration of the sequence galactosyl-galactosyl-xylose-2-phosphate, J. Biol. Chem. 260 (1985) 14722–14726.

[20] M. Ueno, S. Yamada, M. Zako, M. Bernfield, K. Sugahara, Structural characterization of heparan sulfate and chondroitin sulfate of Syndecan-1 purified from normal murine mammary gland epithelial cells. Common phosphorylation of xylose and differential sulfation of galactose in the protein linkage region tetrasaccharide sequence, J. Biol. Chem. 276 (2001) 29134–29140.

[21] J. Moses, Å. Oldberg, F. Cheng, L.Å. Fransson, Biosynthesis of the proteoglycan decorin—transient 2-phosphorylation of xylose during formation of the trisaccharide linkage region, Eur. J. Biochem. 248 (1997) 521–526.

[22] J. Moses, Å. Oldberg, L.Å. Fransson, Initiation of galactosaminoglycan biosynthesis. Separate galactosylation and dephosphorylation pathways for phosphoxylosylated decorin protein and exogenous xyloside, Eur. J. Biochem. 260 (1999) 879–884.

[23] L.C. Pedersen, K. Tsuchida, H. Kitagawa, K. Sugahara, T.A. Darden, M. Negishi, Heparan/chondroitin sulfate biosynthesis. Structure and mechanism of human glucuronyltransferase I, J. Biol. Chem. 275 (2000) 34580–34585.

[24] H. Sakaguchi, M. Watanabe, C. Ueoka, E. Sugiyama, T. Taketomi, S. Yamada, K. Sugahara, Isolation of reducing oligosaccharide chains from the chondroitin/dermatan sulfate-protein linkage region and preparation of analytical probes by fluorescent labeling with 2-aminobenzamide, J. Biochem. 129 (2001) 107–118.

[25] K. Takagaki, A. Kon, H. Kawasaki, T. Nakamura, S. Tamura, M. Endo, Isolation and characterization of Patnopecten mid-gut gland endo-beta-xylosidase active on peptidochondroitin sulfate, J. Biol. Chem. 265 (1990) 854–860.

[26] K. Takagaki, M. Iwafune, I. Kakizaki, K. Ishido, Y. Kato, M. Endo, Cleavage of the xylosyl serine linkage between a core peptide and a glycosaminoglycan chain by cellulases, J. Biol. Chem. 277 (2002) 18397–18403.

[27] Y. Matsuno, M. Kinoshita, K. Kakehi, Electrophoretic analysis of di- and oligosaccharides derived from glycosaminoglycans on microchip format, J. Pharm. Biomed. Anal. 36 (2004) 9–15.

[28] M. Nakano, K. Kakehi, M.H. Tsai, Y.C. Lee, Detailed structural features of glycan chains derived from alpha1-acid glycoproteins of several different animals: The presence of hypersialylated, O-acetylated sialic acids but not disialyl residues, Glycobiology 14 (2004) 431–441.

[29] B.J. Bromke, F. Kueppers, The major urinary protease inhibitor: simplified purification and characterization, Biochem. Med. 27 (1982) 56–67.

[30] Y. Tanaka, S. Maehara, H. Sumi, N. Toki, S. Moriyama, K. Sasaki, Purification and partial characterization of two forms of urinary trypsin inhibitor, Biochim. Biophys. Acta 705 (1982) 192–199.

[31] K. Hochstrasser, O.L. Schonberger, I. Rossmanith, E. Wachter, Kunitz-type proteinase inhibitors derived by limited proteolysis of the inter-alpha-trypsin inhibitor, V. Attachments of carbohydrates in the human urinary trypsin inhibitor isolated by affinity chromatography, Hoppe-Seyler's Z. Physiol. Chem. 362 (1981) 1357–1362.

[32] H. Toyoda, S. Kobayashi, S. Sakamoto, T. Toida, T. Imanari, Structural analysis of a low-sulfated chondroitin sulfate chain in human urinary trypsin inhibitor, Biol. Pharm. Bull. 16 (1993) 945–947.

[33] S. Yamada, M. Oyama, Y. Yuki, K. Kato, K. Sugahara, The uniform galactose 4-sulfate structure in the carbohydrate-protein linkage region of human urinary trypsin inhibitor, Eur. J. Biochem. 233 (1995) 687–693.

[34] N.S. Gunay, K. Tadano-Aritomi, T. Toida, I. Ishizuka, R.J. Linhardt, Evaluation of counterions for electrospray ionization mass spectral analysis of a highly sulfated carbohydrate, sucrose octasulfate, Anal. Chem. 75 (2003) 3226–3231.

[35] P. Flodin, J.D. Gregory, L. Rodén, Separation of acidic oligosaccharides by gel filtration, Anal. Biochem. 8 (1964) 424–433.
[36] R.V. Iozzo, A.D. Murdoch, Proteoglycans of the extracellular environment: clues from the gene and protein side offer novel perspectives in molecular diversity and function, FASEB J. 10 (1996) 598–614.
[37] R.K. Chopra, C.H. Pearson, G.A. Pringle, D.S. Fackre, P.G. Scott, Dermatan sulfate is located on serine-4 of bovine skin proteodermatan sulphate. Demonstration that most molecules possess only one glycosaminoglycan chain and comparison of amino acid sequences around glycosylation sites in different proteoglycans, Biochem. J. 232 (1985) 277–279.
[38] K. Sugahara, Y. Ohkita, Y. Shibata, K. Yoshida, A. Ikegami, Structural studies on the hexasaccharide alditols isolated from the carbohydrate–protein linkage region of dermatan sulfate proteoglycans of bovine aorta, J. Biol. Chem. 270 (1995) 7204–7212.
[39] H. Kitagawa, M. Oyama, K. Masayama, Y. Yamaguchi, K. Sugahara, Structural variations in the glycosaminoglycan–protein linkage region of recombinant decorin expressed in Chinese hamster ovary cells, Glycobiology 7 (1997) 1175–1180.
[40] P.J. Neame, H.U. Choi, L.C. Rosenberg, The primary structure of the core protein of the small, leucine-rich proteoglycan (PG I) from bovine articular cartilage, J. Biol. Chem. 264 (1989) 8653–8661.
[41] F. Cheng, D. Heinegård, A. Malmström, A. Schmidtchen, K. Yoshida, L.Å. Fransson, Pattern of uronosyl epimerization and 4-/6-*O*-sulphation in chondroitin/dermatan sulphate from decorin and biglycan of various bovine tissues, Glycobiology 4 (1994) 685–696.
[42] F.P. Barry, L.C. Rosenberg, J.U. Gaw, T.J. Koob, P.J. Neame, N- and O-linked keratan sulfate on the hyaluronan binding region of aggrecan fron mature and immature bovine cartilage, J. Biol. Chem. 270 (1995) 20516–20524.

Available online at www.sciencedirect.com
SCIENCE DIRECT
ELSEVIER
Journal of Chromatography A, 1103 (2006) 296–306
JOURNAL OF CHROMATOGRAPHY A
www.elsevier.com/locate/chroma

N-linked oligosaccharide analysis of rat brain Thy-1 by liquid chromatography with graphitized carbon column/ion trap-Fourier transform ion cyclotron resonance mass spectrometry in positive and negative ion modes

Satsuki Itoh [a], Nana Kawasaki [a,b,*], Noritaka Hashii [b], Akira Harazono [a], Yukari Matsuishi [a], Takao Hayakawa [c], Toru Kawanishi [a]

[a] *Division of Biological Chemistry and Biologicals, National Institute of Health Science, 1-18-1 Kamiyoga, Setagaya-ku, Tokyo 158-8501, Japan*
[b] *CREST, Japan Science and Technology Agency (JST), Japan*
[c] *Pharmaceutical and Medical Devices Agency, 3-3-2 Kasumigaseki, Chiyoda-ku, Tokyo 100-0013, Japan*

Received 25 July 2005; received in revised form 10 November 2005; accepted 14 November 2005
Available online 20 December 2005

Abstract

We have previously described the site-specific glycosylation analysis of rat brain Thy-1 by LC/multistage tandem mass spectrometry (MS^n) using proteinase-digested Thy-1. In the present study, detailed structures of oligosaccharides released from Thy-1 were elucidated by mass spectrometric oligosaccharide profiling using LC/MS with a graphitized carbon column (GCC–LC/MS). First, using model oligosaccharides, we improved the oligosaccharide profiling by ion trap mass spectrometry (IT–MS) coupled with Fourier transform ion cyclotron resonance mass spectrometry (FT–ICR–MS). Sequential scanning of a full MS^1 scan with FT–ICR–MS followed by data-dependent MS^n with IT–MS in positive ion mode, and a subsequent full MS^1 scan with FT–ICR–MS followed by data-dependent MS^n with IT–MS in negative ion mode enabled the monosaccharide composition analysis as well as profiling and sequencing of both neutral and acidic oligosaccharides in a single analysis. The improved oligosaccharide profiling was applied to elucidation of N-linked oligosaccharides from Thy-1 isolated by sodium dodecyl sulfate-polyacrylamide gel electrophoresis. It was demonstrated that Thy-1 possesses a significant variety of N-linked oligosaccharides, including Lewis a/x, Lewis b/y, and disialylated structure as a partial structure. Our method could be applicable to analysis of a small abundance of glycoproteins, and could become a powerful tool for glycoproteomics.

Keywords: Mass spectrometric oligosaccharide profiling; Graphitized carbon column; Ion trap mass spectrometry; Fourier transform ion cyclotron resonance mass spectrometry; Data-dependent MS^n; Thy-1

1. Introduction

Glycosylation is one of the most abundant post-translational modifications of proteins [1]. It is already known that glycosylation influences the biological functions as well as the physicochemical properties of proteins, i.e., folding, solubility, aggregation, and stability. A number of reports have noted a positive relationship between a change in glycosylation and development, aging, and certain diseases [2–4]. Elucidation of structural detail in oligosaccharides is necessary to clarify the biological properties of glycoproteins.

MS is now a powerful tool for structural analysis of glycoproteins. There are two major mass spectrometric approaches to the structural analysis of glycoproteins, i.e., MS of glycopeptides [5–7] and of oligosaccharides [8–13]. For oligosaccharide sequencing, tandem mass spectrometry as well as exoglycosidase digestions in conjuction with MS is recognized as an effective means of oligosaccharide sequencing [14–16]. Mass spectrometric peptide/glycopeptide mapping by LC coupled with tandem mass spectrometry (LC/MS/MS) is effective for the determination of glycosylation sites and the analysis of site-specific heterogeneity [17–22]. However, structural detail in

* Corresponding author. Division of Biological Chemistry and Biologicals, National Institute of Health Science, 1-18-1, Kamiyoga, Setagaya-ku, Tokyo 158-8501, Japan. Tel.: +81 3 3700 1141; fax: +81 3 3707 6950.
E-mail address: nana@nihs.go.jp (N. Kawasaki).

0021-9673/$ – see front matter © 2005 Elsevier B.V. All rights reserved.
doi:10.1016/j.chroma.2005.11.043

oligosaccharides is not always available by product ion spectra of glycopeptides, as many of the precursor ions consist of uniform peptides carrying different oligosaccharides with identical *m/z* values. LC/MS/MS of glycopeptides has limitations for the structural analysis of carbohydrates due to the difficulty of isolating of glycopeptide isomers. Mass spectrometric oligosaccharide profiling through the separation of isomers by LC can supply the structural detail of each oligosaccharide although it cannot provide information regarding glycosylation sites and site-specific glycosylation [23–29]. MS of both glycopeptides and oligosaccharides is needed for glycosylation analysis of a glycoprotein [30].

Thy-1 is a cell adhesion molecule that belongs to the immunoglobulin superfamily and is attached to the cell membrane via a glycosylphosphatidylinositol (GPI)-anchor. We recently, studied the glycosylation of Thy-1 in rat brain by mass spectrometric peptide/glycopeptide mapping, and demonstrated that Thy-1 possesses various *N*-glycans at Asn23, 74, and 98 [31]. The monosaccharide composition of *N*-glycan at each glycosylation site was estimated by masses of molecular ions; however, structural detail regarding some of the oligosaccharides could not be elucidated by MS^n since many glycopeptides with identical *m/z* values contained several oligosaccharide isomers and yielded product ions from a mixture of these glycopeptide isomers. Mass spectrometric oligosaccharide profiling is necessary for detailed structural analysis of oligosaccharides.

We have previously demonstrated a simple means of oligosaccharide profiling using liquid chromatography/electrospray ionization mass spectrometry with a graphitized carbon column (GCC–LC/MS) [32–34], in which oligosaccharides can be separated on the basis of their branching, sequence, and linkage, and can be characterized based on their monosaccharide compositions estimated from their calculated molecular masses. Here, we study the glycosylation of Thy-1 by oligosaccharide profiling with GCC–LC/MS. First, we improved our oligosaccharide profiling by ion trap mass spectrometry (IT–MS) coupled with Fourier transform ion cyclotron resonance mass spectrometry (FT–ICR–MS). This instrument is capable of both monosaccharide composition analysis by acquisition of accurate masses and data-dependent multistage tandem MS (MS^n) for sequencing with fast switching between positive and negative ion modes. Using a mixture of typical oligosaccharides, including high-mannose-type, and asialo-, trisialylated, and tetrasialylated complex-types, we confirmed that the improved method can be used for monosaccharide composition analysis and detailed structural analysis of both neutral and acidic oligosaccharides. The method was then applied to N-linked oligosaccharide analysis of rat brain Thy-1.

2. Experimental

2.1. Materials

Man7/D1, Man7/D3, and asialo-triantennary (Tri) were obtained from Oxford Glycosystems (Abingdon, UK). Trisialylated triantennary ($TriNA_3$) and tetrasialylated tetraantennary ($TetraNA_4$) were purchased from Dionex (Sunnyvale, CA, USA). Rat brain was purchased from Nippon SLC (Hamamatsu, Japan). Phosphatidylinositol-specific phospholipase C (PIPLC) from *Bacillus cereus* was purchased from Molecular Probes (Eugene, OR, USA). Peptide-*N*-glycosidase F (PNGase F) was purchased from Roche Diagnostics (Mannheim, Germany). SimplyBlue SafeStain was obtained from Invitrogen (Carlsbad, CA, USA).

2.2. Release of N-linked oligosaccharides from rat brain Thy-1 by in-gel PNGase F digestion

PIPLC-treated GPI-anchored proteins were prepared from rat brain as reported previously [31]. Briefly, the homogenate of rat brain was defatted and solubilized with 2% Triton X-114 at 4 °C overnight [35,36]. After centrifugation, the supernatant was subjected to Triton X-114 phase-partitioning at 37 °C. Solubilized membrane proteins in the detergent phase were precipitated with cold acetone, and the precipitates were digested with PIPLC. After resubjecting the digest mixture to Triton X-114 phase-partitioning, PIPLC-treated soluble GPI-anchored proteins in aqueous phase were precipitated by adding cold acetone. These proteins were carboxyamidomethylated [30], and were separated by sodium dodecyl sulfate–polyacrylamide gel electrophoresis (SDS–PAGE) (12.5%) followed by staining with SimplyBlue SafeStain.

In-gel PNGase F digestion of Thy-1 and extraction of N-linked oligosaccharides were performed as previously described

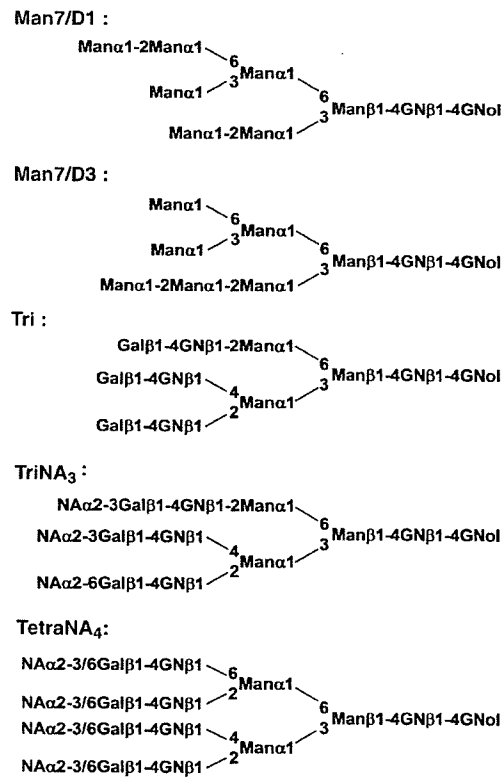

Fig. 1. Structures of major oligosaccharides and their abbreviations. Man: mannose, Gal: galactose, GN; *N*-acetylglucosamine, GNol; *N*-acetylglucosaminitol, NA; *N*-acetylneuramic acid.

[15]. The protein band of Thy-1 (20–25 kDa) was excised, cut into pieces, and destained. The gel pieces were dehydrated with 50% acetonitrile. The dried gels were then equilibrated with 50 mM sodium phosphate buffer (pH 7.2) and incubated at 37 °C with 3 units of PNGase F. The released *N*-glycans were extracted three times from gel pieces by intermittent sonication for 30 min in water. All extracts were combined and lyophilized. The released N-linked oligosaccharides were reduced with $NaBH_4$, as previously reported [33], and subjected to GCC–LC/IT–MS-FT–ICR–MS.

2.3. *N-linked oligosaccharide analysis by GCC–LC/IT–MS-FT–ICR–MS*

GCC–LC/MS was carried out using a MAGIC 2002 system (Michrom BioResource, Auburn, CA, USA) connected to IT–MS instrument coupled with FT–ICR–MS instrument (Finnigan LTQ FT, Thermo Electron Corp., San Jose, CA, USA). The eluents consisted of 5 mM ammonium acetate, pH 9.6, containing 2% CH_3CN (pump A), and 5 mM ammonium acetate, pH 9.6, containing 80% CH_3CN (pump B). The borohydride-reduced N-linked oligosaccharides were separated on Hypercarb (150 mm × 0.2 mm, 5 μm, Thermo Electron Corp.) as GCC with a linear gradient of 5–30% for pump B over a period of 60 min at a flow rate of 2 μl/min.

The MS^n experiment includes sequential scans, as follows: a full MS^1 scan (*m/z* 700–2000) by FT–ICR–MS in positive ion mode, data-dependent MS^n scans by IT–MS for most abundant ions regardless of their charge state, a full MS^1 scan (*m/z* 700–2000) by FT–ICR–MS in negative ion mode, and data-dependent MS^n scans by IT–MS for the most intense ions regardless of their charge state. For the data-dependent MS^n, the following settings were used: the isolation window for precursor masses, ±2.5 Da; collision energy, 35%; dynamic exclusion

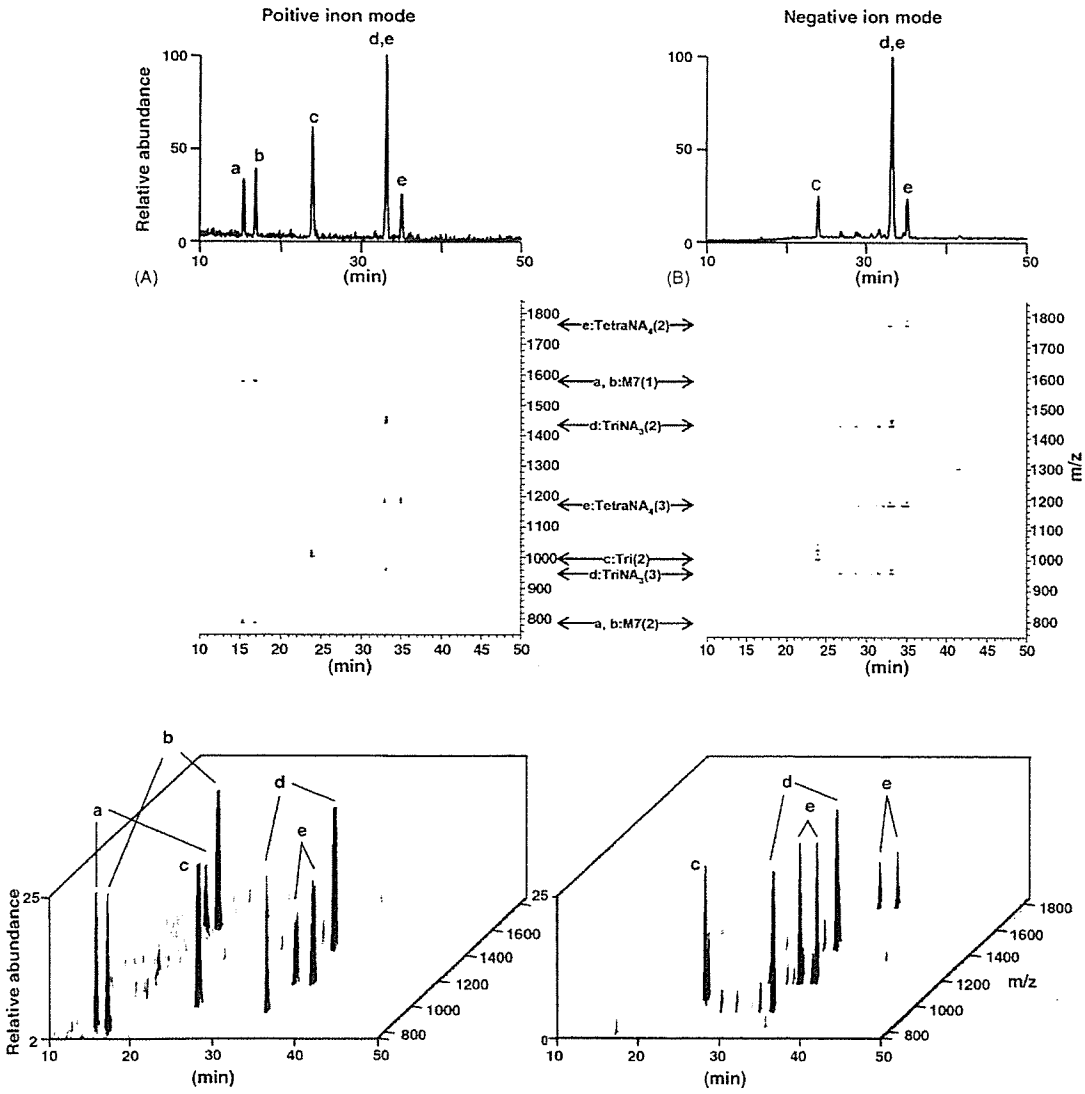

Fig. 2. Typical oligosaccharide profiles obtained by full MS^1 scans with FT–ICR–MS. (A) total ion chromatogram (TIC) (upper), two-dimensional (2D) display (retention time vs. *m/z*) (middle), and three-dimensional (3D) display (lower) in positive ion mode. (B) TIC (upper), 2D (middle) and 3D display (lower) in negative ion mode. Numbers in parentheses after the abbreviation of the model oligosaccharides refer to the charge state.

time, 15 s. The operating conditions employed for LC/MS^n were as follows: tube lens offset, 120 V; capillary voltage, 2.0 kV; and capillary temperature, 200 °C.

3. Results

3.1. GCC–LC/IT–MS-FT–ICR–MS of model oligosaccharides

By using the IT–MS-FT–ICR–MS instrument, the oligosaccharide profiling was shown to be more rapid, accurate, and informative. Man7/D1, Man7/D3, Tri, $TriNA_3$, and $TetraNA_4$, which were chosen as model neutral and acidic oligosaccharides (Fig. 1), were analyzed by alternative scans in positive and negative ion modes, which are consisting of a full MS^1 scan by FT–ICR–MS followed by data-dependent MS^n scans by IT–MS. Fig. 2A and B show the oligosaccharide profiles obtained by a full MS^1 scan with FT–ICR–MS (*m/z* 700–2000) in positive and negative ion modes, respectively. The monosaccharide compositions of individual oligosaccharides could be easily determined by accurate *m/z* values, and the major peaks of a, b, c, d, and e were assigned to Man7/D1 or D3, Man7/D3 or D1, Tri, $TriNA_3$ and $TetraNA_4$, respectively. Oligosaccharides detected at the same *m/z* values are positional isomers. Man7/D1 and D3 were detected in positive ion mode, but were only slightly detectable in negative ion mode. The major isomers of $TriNA_3$ and $TetraNA_4$ were detected in both ion modes, whereas their minor isomers were detected only in negative ion mode. These results demonstrate the advantage of alternative scans in both ion modes.

We confirmed the possibility of data-dependent MS^n scans for sequencing neutral and sialylated oligosaccharides. Man 7/D1 and D3 could be distinguished from each other by data-dependent MS^n (Fig. 3). Oligosaccharide eluted at 15 min could be assigned to Man7/D1 by the relatively intense ions at *m/z* 913 ($Y_{3\alpha}^+$) and 1237 ($Y_{3\beta}^+$), which would be predominantly produced from Man7/D1 by the cleavage of the α1–6-linked or α1–3-linked branch arm of the core mannose (Fig. 3A) (nomenclature proposed by Domon and Costello [37]). Likewise, the oligosaccharide at 17 min could be Man7/D3 based on the intensity of Y_{3x}^+ at *m/z* 1075 generated from Man7/D3 by the cleavages of both the α1–6-linked and α1–3-linked branch arms (Fig. 3B).

Fig. 4A and B show the product ion spectra of $TetraNA_4$ in positive and negative ion modes, respectively. In positive ion mode, the characteristic B ions such as *m/z* 454 (B_{2x}^+), 657 (B_{3x}^+), 1475 (B_{4x}^+), and 1658 (B_6^{2+}), and a ladder of several Y ions with intervals corresponding to Hex, HexNAc, and NeuAc were detected. B/Y ions were also detected at *m/z* 366, 527, 819 (B_5/Y_{3x}^{2+}), and 1330 (B_6/Y_{4x}^{2+}). In negative ion mode, only sialic acids were predominantly eliminated by MS^2 and MS^3. The structural information was provided by MS^4, whereby both B and Y ions were originated from $TetraNA_2$, together with the internal fragmentation ions and cross ring cleaved ions (Fig. 4B). In addition to the B and Y ions, which were predominantly produced in positive ion mode, fragment ions at *m/z* 470 ($C_{2x'}^-$), 1322 ($Z_{6x'}^{2-}$, $[Y_{6x'}\text{-}H_2O]^{2-}$), 1241 ($Z_{5x'}^{2-}$, $[Y_{5x'}\text{-}H_2O]^{2-}$), and 1057 ($Y_{5x''}/Z_{4x'}^{2-}$, $Y_{4x'}/Z_{5x''}^{2-}$, $Y_{4x''}/Z_{5x'}^{2-}$, $Y_{5x'}/Z_{4x''}^{2-}$, $[Y_{4x'/5x''}\text{-}H_2O]^{2-}$, $[Y_{4x''/5x'}\text{-}H_2O]^{2-}$) were detected in negative ion mode. These ions were also useful for the structural characterization of oligosaccharides.

3.2. Glycosylation analysis of Thy-1 by GCC–LC/IT–MS-FT–ICR–MS

The improved oligosaccharide profiling using IT–MS-FT–ICR–MS was applied to the glycosylation analysis of Thy-1. PIPLC-treated Thy-1 in rat brain was isolated by SDS–PAGE [31]. N-linked oligosaccharides were extracted from the gel after in-gel PNGase F digestion and were reduced

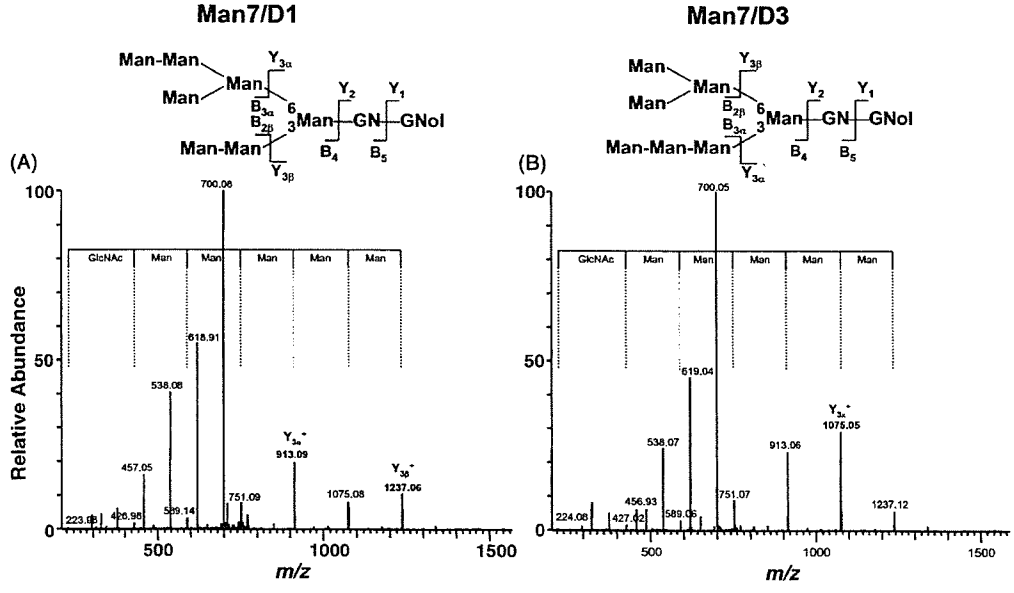

Fig. 3. Product ion spectra of oligosaccharide Man 7/D1 (A) and Man 7/D3 (B).

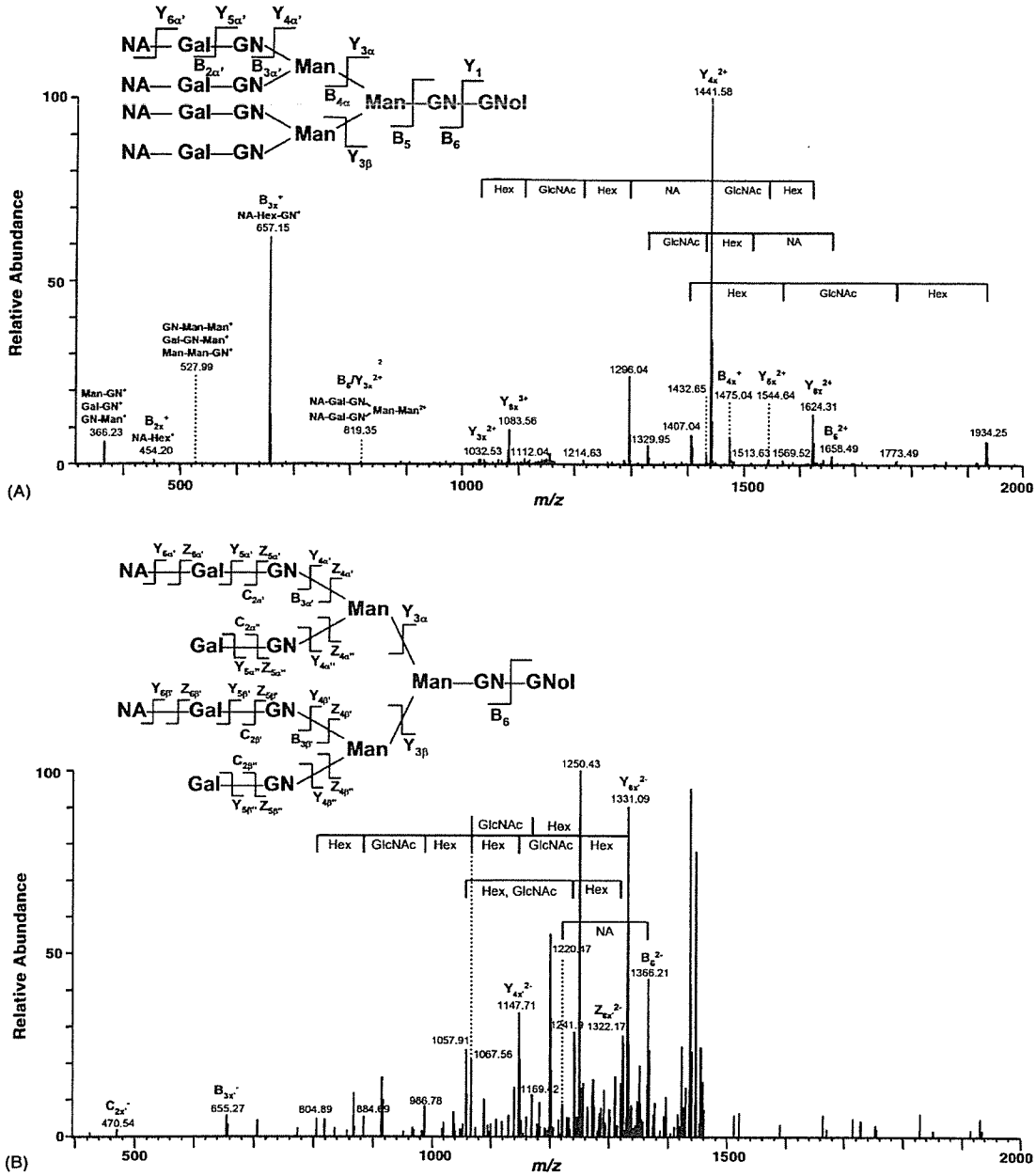

Fig. 4. Product ion spectra of model oligosaccharide, TetraNA$_4$. (A) MS^2 spectrum derived from $[TetraNA_4]^{3+}$ at m/z 1180 in positive ion mode. (B) MS^4 spectrum derived from $[TetraNA_4]^{3-}$ at m/z 1178 → $[TetraNA_3]^{3-}$ at m/z 1081 → $[TetraNA_2]^{2-}$ at m/z 1476 in negative ion mode.

with $NaBH_4$. Fig. 5 shows total ion chromatogram (TIC) (A) obtained by GCC–LC/IT–MS-FT–ICR–MS of borohydrate-reduced oligosaccharides, and two-dimensional display of full MS^1 scans in positive ion mode (red) and negative ion mode (blue) (B), in which oligosaccharides appear as protonated and ammonium adducted forms along with fragment ions. Alternative scanning in potitive and negative ion mode enables us to detect many oligosaccharides without missing less ionized oligosaccharides in either ion mode. For example, oligosaccharides at m/z 762 (2+) and 822 (2+) were detected only in positive ion mode, whereas those at m/z 1387 (2−), 1440 (2−), and 1542 (2−) were detected only in negative ion mode. Furthermore, accurate m/z values acquired by FT–ICR–MS provide their monosaccharide composition, and subsequent data-dependent MS^n allows us to elucidate their monosaccharide sequence as follows.

3.2.1. Monosaccharide composition of oligosaccharides

Oligosaccharides in Thy-1 were assigned to $NeuAc_{0-3}$ $dHex_{0-3}Hex_{3-9}HexNAc_{1-5}HexNAcol_1$ based on their accurate m/z values (Table 1). Oligosaccharides bearing two Fuc residues, in which the m/z values of multiple charged ions are nearly identical to those of oligosaccharides bearing one NeuAc residue instead, could be determined

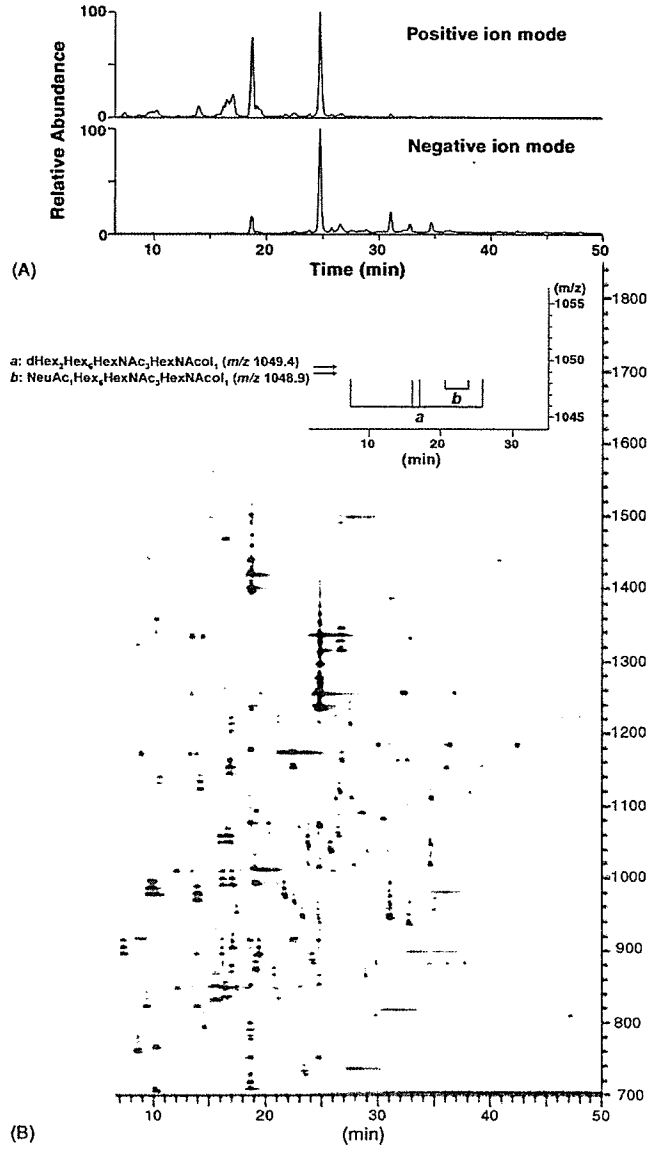

Fig. 5. N-Linked oligosaccharide profile of rat brain Thy-1 obtained by full MS^1 scans with FT–ICR–MS. (A) TIC, and (B) overlapped 2D display in positive (red) and negative (blue) ion modes.

by FT–ICR–MS. For instance, difucosylated oligosaccharides ($dHex_2Hex_6HexNAc_3HexNAcol_1$, theoretical molecular weight: 2096.78 Da) detected at 7.6, 16, 17, and 26 min (Fig. 5, inset, a) were clearly distinguished from monosialylated oligosaccharides ($NeuAc_1Hex_6HexNAc_3HexNAcol_1$, theoretical molecular weight: 2095.76 Da) detected at 21 and 24 min (Fig. 5, inset, b). The improved oligosaccharide profiling indicated that Thy-1 possesses a significant variety of N-linked oligosaccharides containing high-mannose-type (Man5, Man6, Man7, Man8, and M9) and many different complex- and hybrid-type oligosaccharides bearing $NeuAc_{0-3}$ and Fuc_{0-3}. These results are coincident with those of our previous study, in which we carried out mass spectrometric analysis of Thy-1 glycopeptides.

3.2.2. Monosaccharide sequence of oligosaccharides

Monosaccharide sequences of oligosaccharides were elucidated based on the MS/MS spectra. One of the remarkable features of Thy-1 oligosaccharides is the attachment of multiple Fuc and NeuAc residues. We describe below some examples of assignment fucosylated and sialylated oligosaccharides.

3.2.2.1. Gal-(Fuc–)GlcNAc–(Lewis a/x type). Fig. 6A shows the product ion spectrum of a difucosylated oligosaccharide, $dHex_2Hex_4HexNAc_3HexNAcol_1$, at *m/z* 887 (24.3 min) in positive ion mode. There are two possible sites of fucosylation: GlcNAc at the non-reducing end and at the reducing end in the trimannosyl core. The ions detected at *m/z* 350 (Fuc-GlcNAc$^+$, $B_{2\alpha}/Y_{5\alpha'}{}^+$), 370 (Fuc-GlcNAcol$^+$, $Y_{1\alpha}{}^+$), and 512 (Gal-(Fuc–)GlcNAc$^+$, $B_{2\alpha}{}^+$) indicate that Fuc residues link to both the non-reducing end like Lewis a/x, and the inner trimannosyl core GlcNAc. Other ions detected at *m/z* 1553 ($Z_{3\gamma}{}^+$, $[Y_{3\gamma}\text{-}H_2O]^+$) and 1570 ($Y_{3\gamma}{}^+$) suggest a linkage of non-substituted HexNAc at the terminal end. From these characteristic ions together with a Y ion at *m/z* 938.03 ($Y_{3\alpha/3\beta}{}^+$), it can be deduced that this HexNAc is a bisecting GlcNAc that attaches to the core mannose residue via β1–4 linkage. On the basis of these product ions, the oligosaccharide is assigned to the structure indicated in Fig. 6A, inset.

3.2.2.2. Fuc-Gal-(Fuc–)GlcNAc–(Lewis b/y type). Fig. 6B is the product ion spectrum of a difucosylated oligosaccharide, $dHex_2Hex_5HexNAc_4HexNAcol_1$, at *m/z* 1070 (9.2 min). The characteristic ions at *m/z* 512 (Gal-(Fuc–)GlcNAc$^+$, Fuc-Gal-GlcNAc$^+$, $B_{3\alpha'}/Y_{6\alpha'''}{}^+$, $B_{3\alpha'}/Y_{5\alpha''''}{}^+$) and 1915 ($B_6{}^+$) suggest the absence of Fuc at the reducing end GlcNAc; a B ion at *m/z* 658 ($B_{3\alpha'}{}^+$), a B/Y ion at *m/z* 350, and a Y ion at *m/z* 1408 ($Y_{3\beta/4\alpha''}{}^+$) suggest the attachment of two Fuc to Gal-GlcNAc at the non-reducing end, in a similar manner to the Lewis b/y antigen, Fuc-Gal-(Fuc–)GlcNAc–. A Y ion at *m/z* 1936 ($Y_{4\alpha''}{}^+$) indicates a linkage of non-substituted HexNAc at the terminal end. A B/Y ion at *m/z* 877 ($B_{4\alpha}/Y_{5\alpha''''}{}^+$, $B_{4\alpha}/Y_{6\alpha'''}{}^+$) and a Y ion at *m/z* 1610 ($Y_{3\beta}{}^+$) suggest that this non-substituted HexNAc residue is linked to the mannose residue attached to the Fuc-Gal-(Fuc–)GlcNAc– structure. These ions lead to assignment of this oligosaccharide as the structure indicated in Fig. 6B, inset.

3.2.2.3. NeuAc-Gal-(NeuAc–)GlcNAc–. Fig. 7A shows the product ion spectrum of a disialylated oligosaccharide, $NeuAc_2dHex_1Hex_5HexNAc_2HexNAcol_1$, at *m/z* 1085 (30.4 min). Characteristic fragment ions at *m/z* 495 ($B_{3\alpha}/Y_{5\alpha'}{}^+$), 948 ($B_{3\alpha}{}^+$), and 1110 ($B_{4\alpha}{}^+$), together with B ions at *m/z* 453 ($B_{2\alpha'}{}^+$) and 657 ($B_{3\alpha}/Y_{5\alpha''}{}^+$, $B_{3\alpha}/Y_{6\alpha'}{}^+$) suggest the presence of a partial structure of NeuAc-Gal-(NeuAc–)GlcNAc–. Furthermore, detection of Y ions at *m/z* 370 ($Y_{1\alpha}{}^+$) and 1059 ($Y_{3\alpha}{}^+$, $Y_{4\alpha/4\beta}{}^+$) as well as a B ion at *m/z* 1799 ($B_6{}^+$) indicate the linkage of a Fuc residue at the inner trimannosyl core GlcNAc. Based on these product ions, the oligosaccharide detected at *m/z* 1085 was assigned to the structure in Fig. 7A, inset.

Table 1
Summary of N-linked oligosaccharides of rat brain Thy-1

Monosacchardie composition[a]				Theoretical mass[b]	Positive ion mode		Negative ion mnmode		Deduced structure[d]
dHex	Hex	HX	NA		Observed m/z[c]	Retention time (min)	Observed m/z[c]	Retention time (min)	
1	3	2	0	1058.40	1059.46(1)	29.17			CoreF
0	5	2	0	1236.45	1237.47(1)	24.74	1235.45(1)	24.76	M5
0	3	4	0	1318.50	1319.57(1)	8.63			
0	6	2	0	1398.50	1399.53(1)	18.73	1397.50(1)	18.68	M6
0	5	3	0	1439.53	1440.59(1)	9.17			
1	3	4	0	1464.56	733.31(2), 1465.65(1)	23.44			
0	3	5	0	1521.58	761.80(2)	8.63			BisectGN
0	7	2	0	1560.55	781.29(2), 1561.60(1)	18.66			M7
1	5	3	0	1585.59	793.82(2)	14.59			Hybrid
1	5	3	0	1585.59	793.81(2)	19.13			
1	5	3	0	1585.59	793.83(2)	20.96			
0	5	4	0	1642.61	822.33(2)	9.48			Hybrid
0	5	4	0	1642.61	822.33(2)	14.02			
1	3	5	0	1667.64	834.83(2), 1668.69(1)	16.48	832.81(2)	16.44	CoreF
0	4	5	0	1683.63	842.85(2)	17.48			Hybrid
0	8	2	0	1722.61	870.83(2)[e]	17.07			M8
0	5	3	1	1730.62	866.34(2)	20.31			
0	5	3	1	1730.62	866.35(2)	28.91	864.31(2), 1729.64(1)	28.93	Hybrid
2	5	3	0	1731.64	866.86(2)	20.83	864.81(2)	20.85	Hybrid, CoreF, Lax
1	6	3	0	1747.64	874.84(2)	19.19			
2	4	4	0	1772.67	887.37(2)	23.84	885.33(2)	23.86	
2	4	4	0	1772.67	887.36(2)	24.25	885.33(2)	24.27	Hybrid, CoreF, BisectGN
1	5	4	0	1788.67	895.36(2)	7.37			Hybrid
1	5	4	0	1788.67	895.36(2)	13.90			
1	5	4	0	1788.67	895.35(2)	14.16			Hybrid, CoreF
1	5	4	0	1788.67	895.35(2)	19.44	893.33(2)	19.46	Hybrid, CoreF
0	6	4	0	1804.66	903.35(2)	17.07	901.33(2)	17.09	Hybrid, BisectGN
1	4	5	0	1829.69	915.88(2)	8.63			Hybrid
1	4	5	0	1829.69	915.88(2)	9.17			Hybrid
1	4	5	0	1829.69	915.89(2)	18.00			Hybrid
1	4	5	0	1829.69	915.89(2)	22.61	913.84(2)	22.63	
1	5	3	1	1876.68	939.37(2)	21.17	937.34(2)	21.12	
1	5	3	1	1876.68	939.36(2)	24.90	937.34(2)	24.92	
1	5	3	1	1876.68	939.39(2)	32.76	937.33(2)	32.78	Hybrid, CoreF
0	9	2	0	1884.66	951.88(2)[e]	17.53			M9
0	6	3	1	1892.68	947.39(2)	23.31	945.33(2)	23.33	Hybrid
0	6	3	1	1892.68	947.39(2)	31.09	945.33(2)	31.05	Hybrid
2	6	3	0	1893.70	947.87(2)	24.61	945.84(2)	24.70	
1	4	4	1	1917.71			957.85(2)	27.73	
1	4	4	1	1917.71			957.85(2)	28.86	
1	4	4	1	1917.71			957.85(2)	34.91	CoreF
1	4	4	1	1917.71			957.85(2)	35.55	
0	5	4	1	1933.70	967.89(2)	22.61	965.85(2)	22.63	Hybrid
0	5	4	1	1933.70	967.86(2)	24.61	965.82(2)	24.70	
2	5	4	0	1934.72	968.39(2)	13.97			Hybrid
1	6	4	0	1950.72	976.39(2)	9.93			Hybrid, Lax
1	6	4	0	1950.72	976.41(2)	21.76	974.35(2)	21.79	Hybrid, CoreF
2	4	5	0	1975.75	988.90(2)	16.21	986.85(2)	16.16	Complex
2	4	5	0	1975.75	988.90(2)	17.07	986.87(2)	17.09	Complex
0	5	3	2	2021.72			1009.86(2)	26.35	
0	5	3	2	2021.72			1009.85(2)	26.83	
1	6	3	1	2038.73	1020.40(2)	23.84	1018.36(2)	23.80	
1	6	3	1	2038.73	1020.44(2)	27.77	1018.37(2)	27.80	CoreF
1	6	3	1	2038.73	1020.42(2)	34.66	1018.36(2)	34.69	Hybrid, CoreF
1	5	4	1	2079.76	1040.92(2)	25.73	1038.87(2)	25.81	CoreF
1	5	4	1	2079.76	1040.92(2)	29.04	1038.88(2)	28.99	
3	5	4	0	2080.78	1041.42(2)	23.84	1039.39(2)	23.86	
0	6	4	1	2095.76	1048.94(2)	20.57			Hybrid
0	6	4	1	2095.76	1048.91(2)	23.84	1046.87(2)	23.80	Hybrid
2	6	4	0	2096.78	1049.42(2)	7.58			

Table 1 (*Continued*)

Monosaccharide composition[a]				Theoretical mass[b]	Positive ion mode		Negative ion mnmode		Deduced structure[d]
dHex	Hex	HX	NA		Observed *m/z*[c]	Retention time (min)	Observed *m/z*[c]	Retention time (min)	
2	6	4	0	2096.78	1049.42(2)	15.97			
2	6	4	0	2096.78	1049.42(2)	16.61			Hybrid, BisectGN
2	6	4	0	2096.78	1049.43(2)	25.73			
1	7	4	0	2112.77			1055.38(2)	34.62	
1	4	5	1	2120.79	1061.45(2)	20.43			Complex
1	4	5	1	2120.79	1061.45(2)	24.74	1059.39(2)	24.70	
1	4	5	1	2120.79	1061.45(2)	26.47	1059.39(2)	26.42	CoreF
2	5	5	0	2137.80	1069.94(2)	9.17			Lby
2	5	5	0	2137.80	1069.94(2)	21.30			
2	5	5	0	2137.80	1069.95(2)	23.09	1067.9(2)	23.04	
1	5	3	2	2167.78	1084.94(2)	30.41	1082.89(2)	30.37	Hybrid, CoreF
2	4	6	0	2178.83	1090.45(2)	26.08			
0	6	3	2	2183.77	1092.95(2)	28.63	1090.88(2)	28.60	Hybrid, diSia
0	5	4	2	2224.80	1113.45(2)	26.10			
2	5	4	1	2225.82	1113.95(2)	27.56			
2	5	4	1	2225.82	1113.98(2)	34.80			
1	6	4	1	2241.81	1121.95(2)	26.60	1119.90(2)	26.63	
1	6	4	1	2241.81			1119.90(2)	30.58	
1	6	4	1	2241.81			1119.91(2)	38.14	
3	6	4	0	2242.83	1122.46(2)	14.23			
2	7	4	0	2258.83	1130.46(2)	10.47			
3	5	5	0	2283.86	1142.96(2)	16.87			
1	4	6	1	2323.87	1162.98(2)	26.60			
1	6	3	2	2329.83			1163.91(2)	31 72	
1	6	3	2	2329.83			1163.91(2)	32.54	Hybrid, diSia
1	5	4	2	2370.86	1186.55(2)	29.89	1184.42(2)	30.00	Complex, CoreF
1	5	4	2	2370.86			1184.43(2)	36.00	
1	5	4	2	2370.86	1186.52(2)	36.31	1184.42(2)	36.40	Complex, CoreF
1	5	4	2	2370.86	1186.50(2)	42.47	1184.43(2)	42.43	Complex, CoreF
3	5	4	1	2370.86			1184.93(2)	30.99	
2	5	5	1	2428.90	1215.50(2)	21.17	1213.44(2)	21.25	
2	5	5	1	2428.90	1215.50(2)	23.84			
2	5	5	1	2428.90	1215.52(2)	26.32	1213.45(2)	26.28	
2	5	5	1	2428.90	1215.50(2)	27.50	1213.45(2)	27.53	
2	5	4	2	2516.91	1259.60(2)	32.23	1257.45(2)	32.19	Complex, Lax, CoreF, diSia
2	5	4	2	2516.91			1257.45(2)	36.72	
2	5	6	1	2631.98			876.32(3), 1314.99(2)	26.76	
3	5	4	2	2662.97			1330.49(2)	32.78	
1	5	6	2	2777.02			1387.50(2)	30.99	
0	6	5	3	2881.03			1439.50(2)	34.83	
0	6	5	3	2881.03			1439.49(2)	40.77	
2	6	5	2	2882.05			1440.05(2)	37.96	
2	6	6	2	3085.13			1541.55(2)	31.38	

[a] dHex, deoxyhexose; Hex, hexose; HX, *N*-acetylhexamine; NeuAc, *N*-acetylneuramic acid.
[b] Monoisotopic value.
[c] Values in parentheses are charge state.
[d] Structures are deduced by MS^n. Complex, complex-type-oligosaccharide; Hybrid, hybrid-type-oligosaccharide; M5-9, high-mannose-type oligosccharide containing 5–9 mannose residues; BisectGN, bisecting GlcNAc; Lax, Lewis a/x structure; Lby, Lewis b/y structure; diSia, disialic acid.
[e] Ammonium adducted form.

3.2.2.4. NeuAc-Gal-GlcNAc–. Fig. 7B shows the product ion spectrum of a disialylated oligosaccharide, $NeuAc_2dHex_1Hex_5HexNAc_3HexNAcol_1$, at *m/z* 1187 (42.5 min). Although B ions were detected at *m/z* 454 (B_{2x}^+), 657 (B_{3x}^+) and 819 (B_{4x}^+), none of the fragment ions at *m/z* 495 (NeuAc-GlcNAc$^+$), 948 (NeuAc-Gal-(NeuAc–)GlcNAc$^+$), or 1110 (NeuAc-Gal-(NeuAc–)GlcNAc-Man$^+$) were detected in the spectrum. This result suggests that the two NeuAc residues occupy both non-reducing ends of the biantennary form. Fucosylation of the inner trimannnosyl core GlcNAc was determined by the detection of Y ions at *m/z* 370 ($Y_{1\alpha}^+$) and 1059 ($Y_{4\alpha/4\beta}^+$). These product ions lead to assignment of this oligosaccharide the structure in Fig. 6B.

3.2.2.5. (v) NeuAc-NeuAc–. Fig. 7C shows the product ion spectrum of a disialylated and difucosylated oligosaccharide, $NeuAc_2dHex_2Hex_5HexNAc_3HexNAcol_1$, at *m/z* 1260 (32.2 min). The characteristic ions at *m/z* 583 (NeuAc-NeuAc$^+$,

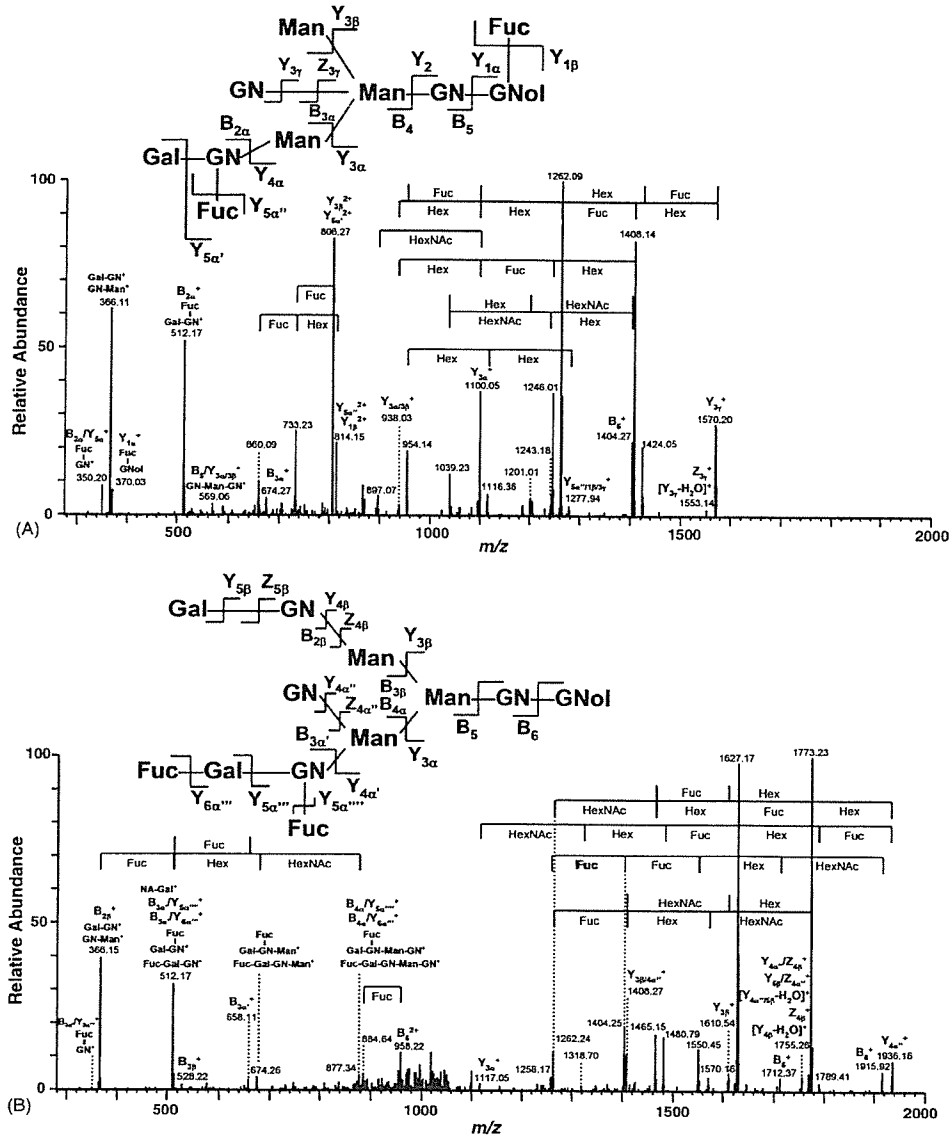

Fig. 6. Product ion spectra of N-linked oligosaccharides of rat brain Thy-1. (A) MS^2 spectrum of $dHex_2Hex_4HexNAc_3HexNAcol_1$ at *m/z* 887 (24.3 min). (B) MS^2 spectrum of $dHex_2Hex_5HexNAc_4HexNAcol_1$ at *m/z* 1070 (9.2 min).

$B_{2\alpha'}{}^+$), 949 (NeuAc-NeuAc-Gal-GlcNAc$^+$, $B_{3\alpha}/Y_{5\alpha''}{}^+$), and 1094 (NeuAc-NeuAc-Gal-(Fuc−)GlcNAc$^+$, $B_{3\alpha}{}^+$) suggest that this oligosaccharide contains a disialic acid residue and one Fuc at the non-reducing end. In addition, a Y ion at *m/z* 370 ($Y_{1\alpha}{}^+$) indicated that the other Fuc was attached to GlcNAc at the reducing end. Based on these product ions, this oligosaccharide structure could be assigned as indicated in Fig. 7C, inset.

4. Discussion

Thy-1 has three *N*-glycosylation sites, Asn23, 74, and 98. We have previously demonstrated the attachment of high-mannose-type, complex-type, and hybrid-type oligosaccharides to these sites. Asn74 is occupied with various *N*-glycans, which have been estimated to be fucosylated and sialylated [31]. Product ion spectra containing fucosylation and sialylation isomers make it difficult to elucidate the detailed structure. We have conducted mass spectrometric oligosaccharide analysis through the separation of diverse oligosaccharides with GCC. We first improved the mass spectrometric oligosaccharide profiling by IT–MS-FT–ICR–MS. The improved method enabled the monosaccharide composition analysis and sequencing of both neutral and acidic oligosaccharides in a single run. Using this method, we successfully analyzed various *N*-glycans of Thy-1 that could not be characterized by the analysis of glycopeptides. We found a Lewis b/y structure and sialylated GlcNAc in the branch structure. Interestingly, disialic acid (NeuAc-NeuAc−), which is known to be involved in neurite formation was found in brain Thy-1 [38].

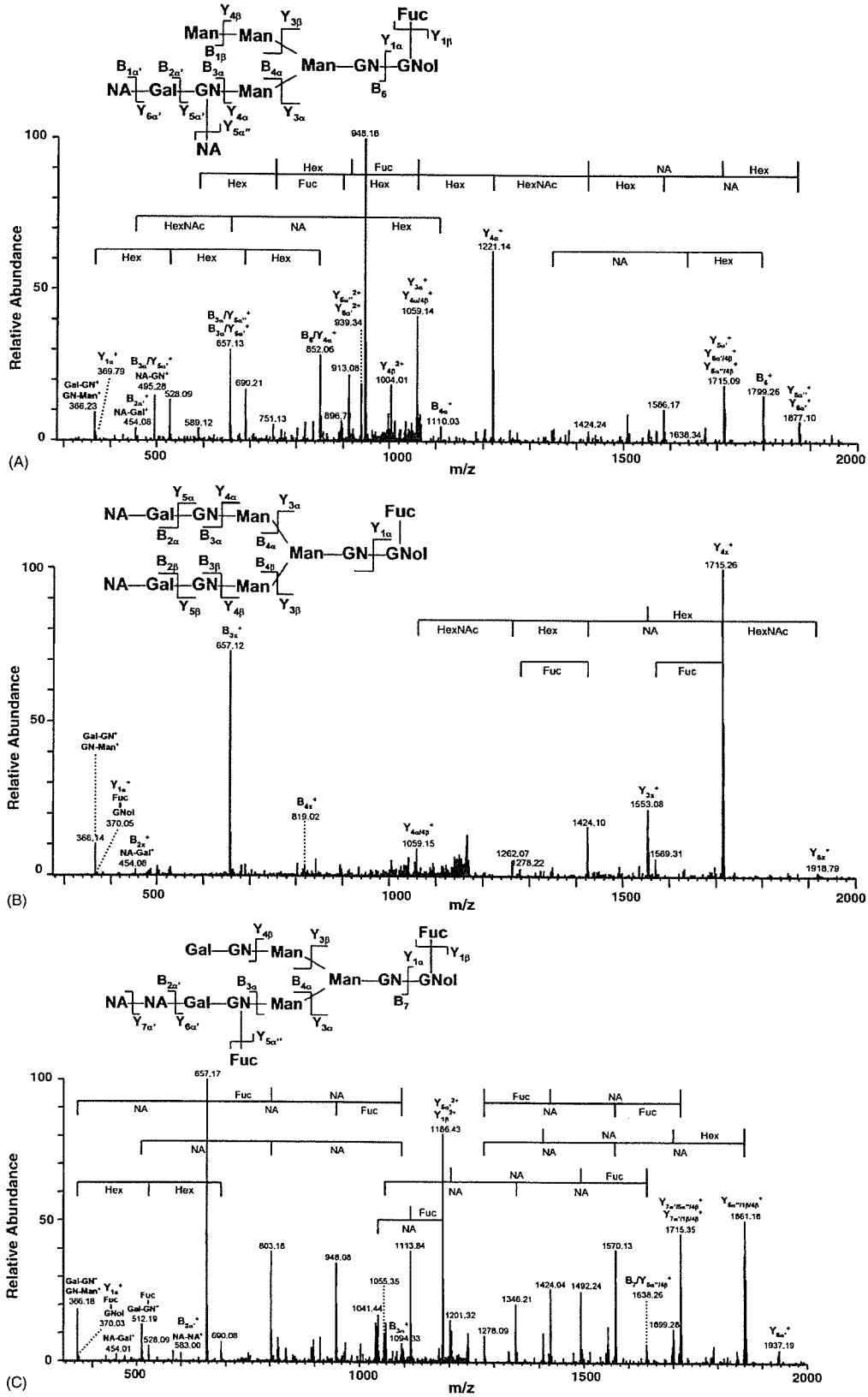

Fig. 7. Product ion spectra of N-linked oligosaccharides of rat brain Thy-1. (A) MS^2 spectrum of $NeuAc_2dHex_1Hex_5HexNAc_2HexNAcol_1$ at *m/z* 1085 (30.4 min). (B) MS^2 spectrum of $NeuAc_2dHex_1Hex_5HexNAc_3HexNAcol_1$ at *m/z* 1187 (42.5 min). (C) MS^2 spectrum of $NeuAc_2dHex_2Hex_5HexNAc_3HexNAcol_1$ at *m/z* 1260 (32.2 min).

In these two studies, we have demonstrated a strategy for glycosylation analysis of Thy-1, including identification of a glycoprotein, determination of glycosylation sites, site-specific glycosylation analysis, and structural analysis of oligosaccharide details. This strategy can be applied to glycosylation analysis of other glycoproteins. Specifically, the glycoprotein sample is divided into two. One is subjected to proteinase digestion followed by peptide/glycopeptide mapping, which provides information on glycosylation sites and site-specific heterogeneity. The other is subjected to PNGase F digestion followed by mass spectrometric oligosaccharide profiling, by which a detailed structure of *N*-glycans released from a glycoprotein could be provided. Recently, proteomic approaches, which are based on two-dimensional electrophoresis followed by mass spectrometry, have been used in various fields. Although glycosylation analysis of abundant glycoproteins in gel has been successful, that of a low-abundance glycoprotein in gel remains a great challenge. The proposed method consisting of peptide/glycopeptide mapping followed by oligosaccharide profiling with sequential scans by IT–MS-FT–ICR–MS will likely be a powerful tool for glycosylation analysis of low-abundance glycoproteins and for proteomics/glycomics.

Acknowledgements

This work was supported in part by a Grant-in-Aid for Creative Scientific Research (16GS0313) from the Ministry of Education, Culture, Sports, and Technology, the Ministry of Health, Labor and Welfare, and Core Research for the Evolutional Science and Technology Program (CREST) of the Japan Science and Technology Agency (JST).

We appreciate Dr. A. Hachisuka of the National Institute of Health Science for her technical advice.

We thank Dr. M. Kubota and Mr. M. Yoshida of Thermo Electron K.K. (Japan) for their technical support.

References

[1] A. Varki, Glycobiology 3 (1993) 97.
[2] J.W. Dennis, M. Granovsky, C.E. Warren, Biochim. Biophys. Acta 1473 (1999) 21.
[3] Y. Sato, M. Kimura, C. Yasuda, Y. Nakano, M. Tomita, A. Kobata, T. Endo, Glycobiology 9 (1999) 655.
[4] G. Durand, N. Seta, Clin. Chem. 46 (2000) 795.
[5] O. Krokhin, W. Ens, K.G. Standing, J. Wilkins, H. Perreault, Rapid Commun. Mass Spectrom. 18 (2004) 2020.
[6] Y. Satomi, Y. Shimonishi, T. Takao, FEBS Lett. 576 (2004) 51.
[7] Y. Wada, M. Tajiri, S. Yoshida, Anal. Chem. 76 (2004) 6560.
[8] W. Chai, V. Piskarev, A.M. Lawson, Anal. Chem. 73 (2001) 651.
[9] D. Sagi, J. Peter-Katalinic, H.S. Conradt, M. Nimtz, J. Am. Soc. Mass Spectrom. 13 (2002) 1138.
[10] A. Zamfir, D.G. Seidler, H. Kresse, J. Peter-Katalinic, Glycobiology 13 (2003) 733.
[11] D.J. Harvey, R.L. Martin, K.A. Jackson, C.W. Sutton, Rapid Commun. Mass Spectrom. 18 (2004) 2997.
[12] C. Robbe, C. Capon, B. Coddeville, J.C. Michalski, Rapid Commun. Mass Spectrom. 18 (2004) 412.
[13] N. Ojima, K. Masuda, K. Tanaka, O. Nishimura, J. Mass Spectrom. 40 (2005) 380.
[14] C.W. Sutton, J.A. O'Neill, J.S. Cottrell, Anal. Biochem. 218 (1994) 34.
[15] B. Küster, S.F. Wheeler, A.P. Hunter, R.A. Dwek, D.J. Harvey, Anal. Biochem. 250 (1997) 82.
[16] B. Küster, T.N. Krogh, E. Mortz, D.J. Harvey, Proteomics 1 (2001) 350.
[17] K. Hirayama, R. Yuji, N. Yamada, K. Kato, Y. Arata, I. Shimada, Anal. Chem. 70 (1998) 2718.
[18] F. Wang, A. Nakouzi, R.H. Angeletti, A. Casadevall, Anal. Biochem. 314 (2003) 266.
[19] K. Sandra, I. Stals, P. Sandra, M. Claeyssens, J. Van Beeumen, B. Devreese, J. Chromatogr. A 1058 (2004) 263.
[20] Y. Satomi, Y. Shimonishi, T. Hase, T. Takao, Rapid Commun. Mass Spectrom. 18 (2004) 2983.
[21] A. Harazono, N. Kawasaki, T. Kawanishi, T. Hayakawa, Glycobiology 15 (2005) 447.
[22] M. Wuhrer, C.A. Koeleman, C.H. Hokke, A.M. Deelder, Anal. Chem. 77 (2005) 886.
[23] B.L. Schulz, N.H. Packer, N.G. Karlsson, Anal. Chem. 74 (2002) 6088.
[24] N.L. Wilson, B.L. Schulz, N.G. Karlsson, N.H. Packer, J. Proteome Res. 1 (2002) 521.
[25] L.A. Gennaro, D.J. Harvey, P. Vouros, Rapid Commun. Mass Spectrom. 17 (2003) 1528.
[26] N.G. Karlsson, B.L. Schulz, N.H. Packer, J. Am. Soc. Mass Spectrom. 15 (2004) 659.
[27] N.G. Karlsson, N.L. Wilson, H.J. Wirth, P. Dawes, H. Joshi, N.H. Packer, Rapid Commun. Mass Spectrom. 18 (2004) 2282.
[28] M. Wuhrer, C.A. Koeleman, A.M. Deelder, C.H. Hokke, Anal. Chem. 76 (2004) 833.
[29] Y. Takegawa, K. Deguchi, S. Ito, S. Yoshioka, H. Nakagawa, S. Nishimura, Anal. Chem. 77 (2005) 2097.
[30] S. Itoh, N. Kawasaki, M. Ohta, T. Hayakawa, J. Chromatogr. A 978 (2002) 141.
[31] S. Itoh, N. Kawasaki, A. Harazono, N. Hashii, Y. Matsuishi, T. Kawanishi, T. Hayakawa, J. Chromatogr. A 1094 (2005) 105.
[32] N. Kawasaki, M. Ohta, S. Hyuga, O. Hashimoto, T. Hayakawa, Anal. Biochem. 269 (1999) 297.
[33] S. Itoh, N. Kawasaki, M. Ohta, M. Hyuga, S. Hyuga, T. Hayakawa, J. Chromatogr. A 968 (2002) 89.
[34] N. Kawasaki, S. Itoh, M. Ohta, T. Hayakawa, Anal. Biochem. 316 (2003) 15.
[35] C. Bordier, J. Biol. Chem. 256 (1981) 1604.
[36] M.P. Lisanti, M. Sargiacomo, L. Graeve, A.R. Saltiel, E. Rodriguez-Boulan, Proc. Natl. Acad. Sci. U.S.A. 85 (1988) 9557.
[37] B. Domon, C.E. Costello, Glycoconjugate J. 5 (1988) 397.
[38] C. Sato, T. Matsuda, K. Kitajima, J. Biol. Chem. 277 (2002) 45299.

Available online at www.sciencedirect.com
SCIENCE DIRECT
Analytical Biochemistry 348 (2006) 259–268
ANALYTICAL BIOCHEMISTRY
www.elsevier.com/locate/yabio

Site-specific N-glycosylation analysis of human plasma ceruloplasmin using liquid chromatography with electrospray ionization tandem mass spectrometry

Akira Harazono *, Nana Kawasaki, Satsuki Itoh, Noritaka Hashii, Akiko Ishii-Watabe, Toru Kawanishi, Takao Hayakawa

National Institute of Health Sciences, Division of Biological Chemistry and Biologicals, 1-18-1 Kami-yoga, Setagaya-Ku, Tokyo 158-8501, Japan

Received 8 June 2005
Available online 10 November 2005

Abstract

Ceruloplasmin has ferroxidase activity and plays an essential role in iron metabolism. In this study, a site-specific glycosylation analysis of human ceruloplasmin (CP) was carried out using reversed-phase high-performance liquid chromatography with electrospray ionization tandem mass spectrometry (LC-ESI-MS/MS). A tryptic digest of carboxymethylated CP was subjected to LC-ESI-MS/MS. Product ion spectra acquired data-dependently were used for both distinction of the glycopeptides from the peptides using the carbohydrate B-ions, such as *m/z* 204 (HexNAc) and *m/z* 366 (HexHexNAc), and identification of the peptide moiety of the glycopeptide based on the presence of the b- and y-series ions derived from the peptide. Oligosaccharide composition was deduced from the molecular weight calculated from the observed mass of the glycopeptide and theoretical mass of the peptide. Of the seven potential N-glycosylation sites, four (Asn119, Asn339, Asn378, and Asn743) were occupied by a sialylated biantennary or triantennary oligosaccharide with fucose residues (0, 1, or 2). A small amount of sialylated tetraantennary oligosaccharide was detected. Exoglycosidase digestion suggested that fucose residues were linked to reducing end GlcNAc in biantennary oligosaccharides and to reducing end and/or α1–3 to outer arms GlcNAc in triantennary oligosaccharides and that roughly one of the antennas in triantennary oligosaccharides was α2–3 sialylated and occasionally α1–3 fucosylated at GlcNAc.

Keywords: Ceruloplasmin; Glycopeptide; Liquid chromatography-electrospray tandem mass spectrometry; Product ion spectrum; Exoglycosidase digestion

Ceruloplasmin (CP)[1] is a blue copper serum glycoprotein synthesized in the liver. CP has ferroxidase activity and plays an essential role in iron metabolism [1–4]. The primary structure of human CP has been determined by amino acid sequencing, and it is composed of a single polypeptide chain of 1046 amino acid residues [5]. The amino acid sequence was confirmed from complete cDNA sequence [6]. The major oligosaccharides in human CP were reported to be sialylated bi- and triantennary structures with or without a fucose residue [7,8]. Although four N-glycosylation sites (Asn119, Asn339, Asn378, and Asn743) were identified among seven potential sites [9], the heterogeneity of oligosaccharides was still unknown at each glycosylation site. CP is an acute phase reactant, and the serum concentration increases during inflammation, infection, and trauma [10]. It is known that the patterns of glycosylation are changed by inflammatory cytokines [11]. Several studies have reported that CP is a good diagnostic marker of solid malignant tumors [12,13] and that the CP glycoform might

* Corresponding author. Fax: +81 3 3700 9084.
E-mail address: harazono@nihs.go.jp (A. Harazono).

[1] *Abbreviations used:* CP, ceruloplasmin; LC-ESI-MS, liquid chromatography with electrospray ionization mass spectrometry; Hex, hexose; HexNAc, *N*-acetylhexosamine; LC-ESI-MS/MS, liquid chromatography with electrospray ionization tandem mass spectrometry; EDTA, ethylenediaminetetraacetic acid; TFA, trifluoroacetic acid; Q-TOF, quadrupole time-of-flight; TIC, total ion chromatogram; NeuAc, *N*-acetylneuraminic acid; GlcNAc, *N*-acetylglucosamine; Fuc, fucose.

0003-2697/$ - see front matter © 2005 Elsevier Inc. All rights reserved.
doi:10.1016/j.ab.2005.10.036